PTEP

Prog. Theor. Exp. Phys. **2016**, 123B04 (27 pages)
DOI: 10.1093/ptep/ptw164

LHC 750 GeV diphoton excess in a radiative seesaw model

Shinya Kanemura[1], Kenji Nishiwaki[2], Hiroshi Okada[3], Yuta Orikasa[2,4], Seong Chan Park[2,5,*] and Ryoutaro Watanabe[6]

[1]*Department of Physics, University of Toyama, 3190 Gofuku, Toyama 930-8555, Japan*
[2]*School of Physics, Korea Institute for Advanced Study, Seoul 02455, Republic of Korea*
[3]*Physics Division, National Center for Theoretical Sciences, National Tsing-Hua University, Hsinchu 30013, Taiwan*
[4]*Department of Physics and Astronomy, Seoul National University, Seoul 08826, Republic of Korea*
[5]*Department of Physics and IPAP, Yonsei University, Seoul 03722, Republic of Korea*
[6]*Center for Theoretical Physics of the Universe, Institute for Basic Science (IBS), Daejeon, 34051, Republic of Korea*
*E-mail: sc.park@yonsei.ac.kr

Received July 20, 2016; Revised October 13, 2016; Accepted October 14, 2016; Published December 19,2016

We investigate a possibility for explaining the recently announced 750 GeV diphoton excess by the ATLAS and CMS experiments at the CERN Large Hadron Collider in a model with multiple doubly charged particles, that was originally suggested for explaining tiny neutrino masses through a three-loop effect in a natural way. The enhanced radiatively generated effective coupling of a new singlet scalar S with diphoton with multiple charged particles in the loop enlarges the production rate of S in $pp \to S + X$ via a photon fusion process and also the decay width $\Gamma(S \to \gamma\gamma)$ even without assuming a tree-level production mechanism. We provide detailed analysis on the cases with or without allowing mixing between S and the standard model Higgs doublet.

Subject Index B46, B54

1. Introduction

In mid-December 2015, both the ATLAS and CMS experiments announced the observation of a new resonance around 750 GeV as a bump in the diphoton invariant mass spectrum from the run-II data in $\sqrt{s} = 13$ TeV [1,2]. Their results are based on the accumulated data of 3.2 fb^{-1} (ATLAS) and 2.6 fb^{-1} (CMS), and local/global significances are $3.9\sigma/2.3\sigma$ (ATLAS) [1] and $2.6\sigma/\lesssim 1.2\sigma$ (CMS) [2], respectively. The best-fit values of the invariant mass are 750 GeV by ATLAS and 760 GeV by CMS, where ATLAS also reported the best-fit value of the total width as 45 GeV.

During/after Moriond EW in March 2016, updated results were reported with the new analysis with different hypotheses on spin (spin-0 or spin-2) and the width to mass ratio ($\Gamma/m < 1\%$ "narrow width" or $\Gamma/m \sim 6$–10% "wide width") [3,4]. Based on the 3.2 fb^{-1} data set, the ATLAS group claimed that the largest deviation from the background-only hypothesis was observed near a mass of 750 GeV, which corresponds to a local excess of 3.9σ for the spin-0 case of $\Gamma \approx 45$ GeV ($\Gamma/m \approx 6\%$). However, we note that the preference for wide width compared with narrow width is only minor by $\sim 0.3\sigma$ significance so that we would take it with caution. In our analysis below, we simply allow both cases with narrow and wide widths. The global significance is still low $\sim 2.0\sigma$.

Funded by SCOAP[3]

On the other hand, based on the upgraded amount of the data of 3.3 fb^{-1}, the CMS group reported a modest excess of events at 760 GeV with a local significance of 2.8–2.9σ depending on the spin hypothesis. The narrow width ($\Gamma/m = 1.4 \times 10^{-2}$) maximizes the local excess. In addition, CMS reported the result of a combined analysis of 8 TeV and 13 TeV data, where the largest excess (3.4σ) was observed at 750 GeV for the narrow width ($\Gamma/m = 1.4 \times 10^{-4}$). The global significances are $< 1\sigma$ (1.6σ) in the 13 TeV (8 TeV + 13 TeV) analyses, respectively. No official combined (ATLAS & CMS) result has been made so far.

Just after the advent of the first announcement, various ways to explain the 750 GeV excess were proposed, even within December 2015, in Refs. [5–125]. The first unofficial interpretation of the excess in terms of the signal strength of a scalar (or a pseudoscalar) resonance S, $pp \to S + X \to \gamma\gamma + X$, was made immediately after the first announcement in Ref. [11] based on the expected and observed exclusion limits in both of the experiments. The authors claimed

$$\mu^{\rm ATLAS}_{13\ {\rm TeV}} = \sigma(pp \to S + X)_{13\ {\rm TeV}} \times \mathcal{B}(S \to \gamma\gamma) = (10^{+4}_{-3})\ {\rm fb}, \tag{1.1}$$

$$\mu^{\rm CMS}_{13\ {\rm TeV}} = \sigma(pp \to S + X)_{13\ {\rm TeV}} \times \mathcal{B}(S \to \gamma\gamma) = (5.6 \pm 2.4)\ {\rm fb}, \tag{1.2}$$

with a Poissonian likelihood function (for the ATLAS measurement) and a Gaussian approximation (for the CMS measurement), respectively.

On the other hand, both the ATLAS and CMS groups reported that no significant excess over the standard model (SM) background was observed in their analyses based on the run-I data at $\sqrt{s} = 8$ TeV [126,127], while a mild upward bump was found in the CMS data around 750 GeV. In Ref. [11], the signal strengths at $\sqrt{s} = 8$ TeV were extracted by use of the corresponding expected and observed exclusion limits given by the experiments, in the Gaussian approximation, for a narrow-width scalar resonance as

$$\mu^{\rm ATLAS}_{8\ {\rm TeV}} = \sigma(pp \to S + X)_{8\ {\rm TeV}} \times \mathcal{B}(S \to \gamma\gamma) = (0.46 \pm 0.85)\ {\rm fb}, \tag{1.3}$$

$$\mu^{\rm CMS}_{8\ {\rm TeV}} = \sigma(pp \to S + X)_{8\ {\rm TeV}} \times \mathcal{B}(S \to \gamma\gamma) = (0.63 \pm 0.35)\ {\rm fb}. \tag{1.4}$$

It is mentioned that when we upgrade the collider energy from 8 TeV to 13 TeV, a factor 4.7 enhancement is expected [11,128], when the resonant particle is produced via gluon fusion, and then the data at $\sqrt{s} = 8$ TeV and 13 TeV are compatible at around the 2σ confidence level (C.L.). Indeed, in the second announcement [3], the ATLAS group discussed this point based on the reanalyzed 8 TeV data corresponding to an integrated luminosity of 20 fb^{-1} with the latest photon energy calibration in the run-I, which is close to the calibration used for the 13 TeV data. When $m = 750$ GeV and $\Gamma/m = 6\%$, the difference between the 8 TeV and 13 TeV results corresponds to statistical significances of 1.2σ (2.1σ) if gluon–gluon (quark–antiquark) productions are assumed. These observations would give us a stimulating hint for surveying the structure of physics beyond the SM above the electroweak scale even though the accumulated amount of data would not be enough for detailed discussions and the errors are large at the present stage.

A key point to understand the resonance is the fact that no bump around 750 GeV has been found in the other final states in either the 8 TeV or 13 TeV data. If $\mathcal{B}(S \to \gamma\gamma)$ is the same as the 750 GeV Higgs one, $\mathcal{B}(h \to \gamma\gamma)|_{750\,{\rm GeV\,SM}} = 1.79 \times 10^{-7}$ [129], we can immediately recognize that such a possibility is inconsistent with the observed results, e.g., in the ZZ final state, at $\sqrt{s} = 8$ TeV, where the significant experimental 95% C.L. upper bound on the ZZ channel is 12 fb by ATLAS [130] and the branching ratio $\mathcal{B}(h \to ZZ)|_{750\,{\rm GeV\,SM}} = 0.290$ [129]. In general, the process $S \to \gamma\gamma$ should be loop induced since S has zero electromagnetic charge and then the value of $\mathcal{B}(S \to \gamma\gamma)$ tends to

be suppressed because tree-level decay branches generate primary components of the total width of S. Then, a reasonable setup for explaining the resonance consistently is that all of the decay channels of S are one loop induced, where S would be a gauge singlet under $SU(3)_C$ and $SU(2)_L$ since a nonsinglet gauge assignment leads to tree-level gauge interactions, which are not desirable in our case.

An example of this direction is that S is a singlet scalar and it couples to vector-like quarks, which contribute to both $pp \to S + X$ and $S \to \gamma\gamma$ via gluon fusion and photon fusion, respectively. The possibility of diphoton production solely due to photon fusion is also an open possibility as discussed in Refs. [34,40] in the context of the 750 GeV excess. The basic idea is simple: when a model contains multiple $SU(2)_L$ singlet particles with large $U(1)_Y$ hypercharges, the magnitude of the photon fusions in the production and decay sequences is largely enhanced.

In this paper, we focus on the radiative seesaw models [131–135], especially where neutrino masses are generated at the three-loop level [136–153]. In such scenarios, multiple charged scalars are introduced for realizing the three-loop origin of the neutrino mass, (distinct from the models with one or two loops). We show that when these charged scalars couple to the singlet S strongly enough, we can achieve a reasonable amount of the production cross section in $pp \to S + X \to \gamma\gamma + X$ through photon fusion. Concretely, we start from the three-loop model [150], and extend the model with additional charged scalars to explain the data.[1]

This paper is organized as follows. In Sect. 2, we introduce our model based on the model for three-loop induced neutrino masses. In Sect. 3, we show detail of the analysis and numerical results. Section 4 is devoted to summary and discussions.

2. Model

Multiple (doubly) charged particles would induce a large radiative coupling with a singlet scalar S with $\gamma\gamma$ via one-loop diagrams. We may find the source from multi-Higgs models or extra dimensions [160–177] but here we focus on a model for radiative neutrino masses, recently suggested by some of the authors [150] as a benchmark model, which can be extended with a singlet scalar S for the 750 GeV resonance.

2.1. Review: A model for three-loop induced neutrino mass

Our strategy is based on the three-loop induced radiative neutrino model with a $U(1)$ global symmetry [150], where we introduce three Majorana fermions $N_{R_{1,2,3}}$ and new bosons: one gauge-singlet neutral boson Σ_0, two singly charged singlet scalars $(h_1^\pm, h_2^\pm)$, and one gauge-singlet doubly charged boson $k^{\pm\pm}$ to the SM. The particle contents and their charges are shown in Table 1.

We assume that only the SM-like Higgs Φ and the additional neutral scalar Σ_0 have VEVs, which are symbolized by $\langle\Phi\rangle \equiv v/\sqrt{2}$ and $\langle\Sigma_0\rangle \equiv v'/\sqrt{2}$, respectively. Here, $x\,(\neq 0)$ is an arbitrary number of the charge of the hidden $U(1)$ symmetry, and under the assignments, neutrino mass matrix is generated at the three-loop level, with a schematic picture shown in Fig. 1. A remnant Z_2 symmetry remains after the hidden $U(1)$ symmetry breaking and the particles $N_{R_{1,2,3}}$ and $h_2^\pm$ have negative parities. Then, when a Majorana neutrino is the lightest among them, it becomes a dark matter (DM) candidate and the stability is accidentally ensured.

[1] Recently, several other works have emerged in this direction [154–159].

Table 1. Contents of lepton and scalar fields and their charge assignment under $SU(3)_C \times SU(2)_L \times U(1)_Y \times U(1)$, where $U(1)$ is an additional global symmetry and $x \neq 0$. The subscripts found in the lepton fields i (= 1, 2, 3) indicate generations of the fields. The bold letters emphasize that these numbers correspond to representations of the Lie groups of the NonAbelian gauge interactions. The scalar particles shown in the right category (New Scalar Fields) are added to the original model proposed in Ref. [150] to explain the 750 GeV excess.

	Lepton fields			Scalar fields					New scalar fields	
Characters	L_{L_i}	e_{R_i}	N_{R_i}	Φ	Σ_0	h_1^+	h_2^+	k^{++}	j_a^{++}	S
$SU(3)_C$	**1**	**1**	**1**	**1**	**1**	**1**	**1**	**1**	**1**	**1**
$SU(2)_L$	**2**	**1**	**1**	**2**	**1**	**1**	**1**	**1**	**1**	**1**
$U(1)_Y$	$-1/2$	-1	0	$1/2$	0	1	1	2	2	0
$U(1)$	0	0	$-x$	0	$2x$	0	x	$2x$	$2x$	0

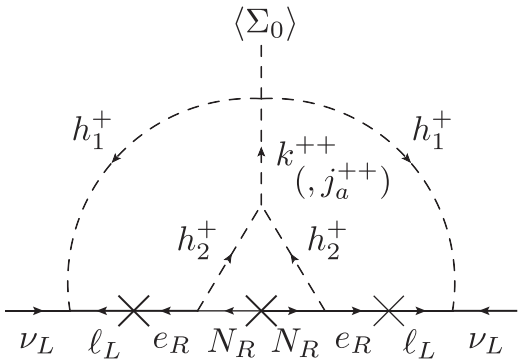

Fig. 1. A schematic description for the radiative generation of neutrino masses.

In the original model, the Lagrangian of the Yukawa sector $\mathcal{L}_Y$ and the scalar potential $\mathcal{V}$, allowed under the gauge and global symmetries, are given as

$$-\mathcal{L}_Y = (y_\ell)_{ij}\bar{L}_{L_i}\Phi e_{R_j} + \tfrac{1}{2}(y_L)_{ij}\bar{L}^c_{L_i}L_{L_j}h_1^+ + (y_R)_{ij}\bar{N}_{R_i}e^c_{R_j}h_2^- + \tfrac{1}{2}(y_N)_{ij}\Sigma_0\bar{N}^c_{R_i}N_{R_j} + \text{h.c.}, \tag{2.1}$$

$$\begin{aligned}\mathcal{V} = {} & m_\Phi^2|\Phi|^2 + m_\Sigma^2|\Sigma_0|^2 + m_{h_1}^2|h_1^+|^2 + m_{h_2}^2|h_2^+|^2 + m_k^2|k^{++}|^2 \\ & + \left[\lambda_{11}\Sigma_0^* h_1^- h_1^- k^{++} + \mu_{22}h_2^+h_2^+k^{--} + \text{h.c.}\right] + \lambda_\Phi|\Phi|^4 + \lambda_{\Phi\Sigma}|\Phi|^2|\Sigma_0|^2 + \lambda_{\Phi h_1}|\Phi|^2|h_1^+|^2 \\ & + \lambda_{\Phi h_2}|\Phi|^2|h_2^+|^2 + \lambda_{\Phi k}|\Phi|^2|k^{++}|^2 + \lambda_\Sigma|\Sigma_0|^4 + \lambda_{\Sigma h_1}|\Sigma_0|^2|h_1^+|^2 + \lambda_{\Sigma h_2}|\Sigma_0|^2|h_2^+|^2 \\ & + \lambda_{\Sigma k}|\Sigma_0|^2|k^{++}|^2 + \lambda_{h_1}|h_1^+|^4 + \lambda_{h_1h_2}|h_1^+|^2|h_2^+|^2 + \lambda_{h_1k}|h_1^+|^2|k^{++}|^2 \\ & + \lambda_{h_2}|h_2^+|^4 + \lambda_{h_2k}|h_2|^2|k^{++}|^2 + \lambda_k|k^{++}|^4,\end{aligned} \tag{2.2}$$

where the indices i,j indicate matter generations and the superscript "c" means charge conjugation (with the $SU(2)_L$ rotation by $i\sigma_2$ for $SU(2)_L$ doublets). We assume that y_N is diagonal, where the right-handed neutrino masses are calculated as $M_{N_i} = \frac{v'}{\sqrt{2}}(y_N)_{ii}$ with the assumed ordering $M_{N_1}(=\text{DM mass}) < M_{N_2} < M_{N_3}$. The neutral scalar fields are shown in the unitary gauge as

$$\Phi = \begin{bmatrix} 0 \\ \frac{v+\phi}{\sqrt{2}} \end{bmatrix}, \quad \Sigma_0 = \frac{v'+\sigma}{\sqrt{2}}\exp(iG/v'), \tag{2.3}$$

with $v \simeq 246$ GeV and an associated Nambu–Goldstone (NG) boson G via the global $U(1)$ breaking due to the occurrence of nonzero v'. Requiring the tadpole conditions, $\partial\mathcal{V}/\partial\phi|_{\phi=v} = \partial\mathcal{V}/\partial\sigma$

$|_{\sigma=v'}=0$, the resultant mass matrix squared of the charge conjugation parity (CP) even components (ϕ,σ) is given by

$$m^2(\phi,\sigma)=\begin{bmatrix}2\lambda_\Phi v^2 & \lambda_{\Phi\Sigma}vv'\\ \lambda_{\Phi\Sigma}vv' & 2\lambda_\Sigma v'^2\end{bmatrix}=\begin{bmatrix}\cos\alpha & \sin\alpha\\ -\sin\alpha & \cos\alpha\end{bmatrix}\begin{bmatrix}m_h^2 & 0\\ 0 & m_H^2\end{bmatrix}\begin{bmatrix}\cos\alpha & -\sin\alpha\\ \sin\alpha & \cos\alpha\end{bmatrix}, \tag{2.4}$$

where h is the SM-like Higgs ($m_h=125$ GeV) and H is an additional CP even Higgs mass eigenstate. The mixing angle α is determined as

$$\sin 2\alpha=\frac{2\lambda_{\Phi\Sigma}vv'}{m_H^2-m_h^2}. \tag{2.5}$$

The neutral bosons ϕ and σ are represented in terms of the mass eigenstates h and H as

$$\phi=h\cos\alpha+H\sin\alpha,\quad \sigma=-h\sin\alpha+H\cos\alpha. \tag{2.6}$$

The two CP even scalars h and H could work as DM-portal scalars and participate in the DM pair annihilation. The mass eigenvalues for the singly charged bosons $h_1^\pm$, $h_2^\pm$ and the doubly charged boson $k^{\pm\pm}$ are given as

$$m^2_{h_1^\pm}=m^2_{h_1}+\tfrac{1}{2}(\lambda_{\Phi h_1}v^2+\lambda_{\Sigma h_1}v'^2),\quad m^2_{h_2^\pm}=m^2_{h_2}+\tfrac{1}{2}(\lambda_{\Phi h_2}v^2+\lambda_{\Sigma h_2}v'^2),$$
$$m^2_{k^{\pm\pm}}=m^2_k+\tfrac{1}{2}(\lambda_{\Phi k}v^2+\lambda_{\Sigma k}v'^2). \tag{2.7}$$

This model can explain the smallness of the observed neutrino masses and the presence of DM without severe parameter tuning. A summary of the features in the model is given in Appendix A.

Here we introduce a real singlet scalar S in the model and assume that it couples with the doubly charged scalar(s). Due to the contributions of the charged particles in the loop, a large branching ratio $\mathcal{B}(S\to\gamma\gamma)$ is achievable without assuming tree-level interactions [34,40]. When $\mathcal{B}(S\to\gamma\gamma)$ is sizable, the production cross section of the resonance particle, $\sigma(pp\to S+X)$, becomes large through photon fusion processes; thus we do not have to rely on gluon fusion processes, which often request additional colored particles that bring in dangerous hadronic activities. Thus we may explain the 750 GeV excess as pointed out in Refs. [34,40].

2.2. *Extension with a scalar S for the 750 GeV resonance*

In the following part, we consider an extension of the original model with the new interactions as

$$\begin{aligned}\Delta\mathcal{V}=&\,\hat\mu_{Sk}S|k^{++}|^2+\hat\lambda_{Sk}S^2|k^{++}|^2+\mathcal{V}(S)\\&+\sum_{a=1}^{N_j}\Big\{\hat m^2_{j_a^{\pm\pm}}|j_a^{++}|^2+\hat\mu_{Sj_a}S|j_a^{++}|^2+\hat\lambda_{Sj_a}S^2|j_a^{++}|^2\\&+\Big[\lambda_{11}^{(a)}\Sigma_0^*h_1^-h_1^-j_a^{++}+\mu_{22}^{(a)}h_2^+h_2^+j_a^{--}+\text{h.c.}\Big]\Big\},\end{aligned} \tag{2.8}$$

where S is a real scalar and $j_a^{\pm\pm}$ $(a=1,2,\ldots,N_j)$ are additional $\mathrm{SU}(2)_L$ singlet doubly charged scalars with hypercharge $+2$ and a global $U(1)$ charge $+2x$. Here, $\mathcal{V}(S)$ represents the potential of the singlet scalar S. Here, we assume that S has a VEV, and S should be replaced with $S\to\langle S\rangle+S$.

After the replacement, we pick up the relevant terms for our analysis and summarize:

$$\Delta\mathcal{V}_{\rm eff} = \mu_{Sk} S|k^{++}|^2 + \frac{1}{2}m_S^2 S^2 + \sum_{a=1}^{N_j}\left\{m^2_{j_a^{\pm\pm}}|j_a^{++}|^2 + \mu_{Sj_a}S|j_a^{++}|^2 + \left[\lambda_{11}^{(a)}\Sigma_0^* h_1^- h_1^- j_a^{++} + \mu_{22}^{(a)} h_2^+ h_2^+ j_a^{--} + \text{h.c.}\right]\right\}, \quad (2.9)$$

with

$$m^2_{j_a^{\pm\pm}} \equiv \hat{m}^2_{j_a^{\pm\pm}} + \hat{\mu}_{Sj_a}\langle S\rangle + \hat{\lambda}_{Sj_a}\langle S\rangle^2,$$
$$\mu_{Sk} \equiv \hat{\mu}_{Sk} + 2\hat{\lambda}_{Sk}\langle S\rangle, \quad \mu_{Sj_a} \equiv \hat{\mu}_{Sj_a} + 2\hat{\lambda}_{Sj_a}\langle S\rangle. \quad (2.10)$$

The squared physical masses of S and $j_a^{\pm\pm}$ are m_S^2 and $m^2_{j_a^{\pm\pm}}$, respectively and we set m_S to 750 GeV for our explanation of the 750 GeV excess.[2] Here, $j_a^{\pm\pm}$ has the same charges as $k^{\pm\pm}$ and then can contribute to the three-loop induced neutrino masses shown in Fig. 1.[3] The trilinear terms in the square brackets are required for evading the stability of $j_a^{\pm\pm}$. We also ignore such possible terms as $|j_a^{++}|^2|\Phi|^2$, $|j_a^{++}|^2|\Sigma_0|^2$ and $S|\Phi|^2$, $S|\Sigma_0|^2$ in Eq. (2.8) in our analysis below. This is justified as a large VEV of S generates large effective trilinear couplings μ_{Sk} and μ_{Sj_a} through the original terms $S^2|k^{++}|$ and $S^2|j_a^{++}|$, respectively, even when the dimensionless coefficients $\hat{\lambda}_{Sk}$ and $\hat{\lambda}_{Sj_a}$ are not large.

3. Analysis

3.1. *Formulation of* $p(\gamma)p(\gamma) \to S + X \to \gamma\gamma + X$

Additional interactions in Eq. (2.9) provide possible decay channels of S to $\gamma\gamma$, $Z\gamma$, ZZ, and $k^{++}k^{--}$ or $j_a^{++}j_a^{--}$ up to the one-loop level. We assume that $m_{k^{\pm\pm}}$ and $m_{j_a^{\pm\pm}}$ are greater than $m_S/2$ ($= 375$ GeV), where the last two decay channels at the tree level are closed kinematically. Here, we show the case when S is a mass eigenstate and there is no mixing through mass terms with other scalars. In the present case that no tree-level decay branch is open and only $\mathrm{SU}(2)_L$ singlet charged scalars describe the loop-induced partial widths, the relative strengths among $\Gamma_{S\to\gamma\gamma}$, $\Gamma_{S\to Z\gamma}$, $\Gamma_{S\to ZZ}$, and $\Gamma_{S\to W^+W^-}$ are governed by quantum numbers at the one-loop level[4] as

$$\Gamma_{S\to\gamma\gamma} : \Gamma_{S\to Z\gamma} : \Gamma_{S\to ZZ} : \Gamma_{S\to W^+W^-} \approx 1 : 2\left(\frac{s_{\rm W}^2}{c_{\rm W}^2}\right) : \left(\frac{s_{\rm W}^4}{c_{\rm W}^4}\right) : 0. \quad (3.1)$$

In the following, we calculate $\Gamma_{S\to ZZ}$ in a simplified way:

$$\Gamma_{S\to ZZ} \approx \frac{s_{\rm W}^2}{2c_{\rm W}^2}\Gamma_{S\to Z\gamma} \simeq 0.15\,\Gamma_{S\to Z\gamma}. \quad (3.2)$$

Here, we represent a major part of partial decay widths of S with our notation for loop functions with the help of Refs. [179–184]. In the following part, for simplicity, we set all the masses of the

[2] In a later part of Sect. 3.2.2, we have discussions on the situation when S and Φ are mixed.

[3] In general, mixing between $k^{\pm\pm}$ and $j_a^{\pm\pm}$ could be allowed but the induced value via the renormalization group running at the scale of our interest is expected to be small with heavy masses of $h_1^\pm$ and $h_2^\pm$, thus is neglected.

[4] The branching fractions are easily understood in an effective theory with the standard model gauge symmetries. See, e.g., [178] with $s_2 = 0$ in the paper.

doubly charged scalars $m_{j_a^{\pm\pm}}$ the same as $m_{k^{\pm\pm}}$, while we ignore the contributions from the two singly charged scalars $h^{\pm}_{1,2}$ since they should be at least as heavy as around 3 TeV and decoupled as mentioned in Appendix A. The concrete forms of $\Gamma_{S\to\gamma\gamma}$ and $\Gamma_{S\to Z\gamma}$ are

$$\Gamma_{S\to\gamma\gamma} = \frac{\alpha_{\rm EM}^2 m_S^3}{256\pi^3 v^2}\left|\frac{1}{2}\frac{v\mu}{m_{k^{\pm\pm}}^2}Q_k^2 A_0^{\gamma\gamma}(\tau_k)\right|^2, \tag{3.3}$$

$$\Gamma_{S\to Z\gamma} = \frac{\alpha_{\rm EM}^2 m_S^3}{512\pi^3}\left(1-\frac{m_Z^2}{m_S^2}\right)^3\left|-\frac{\mu}{m_{k^{\pm\pm}}^2}(2Q_k g_{Zkk})A_0^{Z\gamma}(\tau_k,\lambda_k)\right|^2, \tag{3.4}$$

with

$$\mu = \Sigma_a \mu_a \equiv \left[\mu_{Sk} + \sum_{a=1}^{N_j}\mu_{Sj_a}\right], \quad g_{Zkk} = -Q_k\left(\frac{s_{\rm W}}{c_{\rm W}}\right), \quad \tau_k = \frac{4m_{k^{\pm\pm}}^2}{m_S^2}, \quad \lambda_k = \frac{4m_{k^{\pm\pm}}^2}{m_Z^2}. \tag{3.5}$$

Here, Q_k $(=2)$ is the electric charge of the doubly charged scalars in units of the positron's one, $c_{\rm W}$ and $s_{\rm W}$ are the cosine and the sine, respectively, of the Weinberg angle $\theta_{\rm W}$, and $\alpha_{\rm EM}$ is the electromagnetic fine structure constant. In the following calculation, we use $s_{\rm W}^2 = 0.23120$ and $\alpha_{\rm EM} = 1/127.916$. The loop factors take the following forms,:

$$\begin{aligned} A_0^{\gamma\gamma}(x) &= -x^2\left[x^{-1} - f(x^{-1})\right], \\ A_0^{Z\gamma}(x,y) &= \frac{xy}{2(x-y)} + \frac{x^2y^2}{2(x-y)^2}\left[f(x^{-1}) - f(y^{-1})\right] + \frac{x^2y}{(x-y)^2}\left[g(x^{-1}) - g(y^{-1})\right]. \end{aligned} \tag{3.6}$$

The two functions $f(z)$ and $g(z)$ ($z \equiv x^{-1}$ or y^{-1}) are formulated as

$$f(z) = \arcsin^2\sqrt{z} \quad \text{for } z \le 1, \tag{3.7}$$

$$g(z) = \sqrt{z^{-1}-1}\arcsin\sqrt{z} \quad \text{for } z \le 1, \tag{3.8}$$

where the situation $m_S \le 2m_{k^{\pm\pm}}$, $m_Z \le 2m_{k^{\pm\pm}}$ corresponds to $z \le 1$. For simplicity, we assume the relation

$$\mu_{Sk} = \mu_{Sj_a}, \tag{3.9}$$

for all a.

For the production of S corresponding to the 750 GeV resonance, we consider the photon fusion process, as first discussed in the context of the 750 GeV excess in Refs. [34,40]. We take the photon parton distribution function (PDF) from Ref. [185], which adopted the methods in Ref. [186].[5] The inclusive production cross section of a scalar (or pseudoscalar) resonance R is generally formulated as

$$\frac{d\sigma^{\rm inc}(p(\gamma)p(\gamma)\to R+X)}{dM_R^2\,dy_R} = \frac{d\mathcal{L}^{\rm inc}}{dM_R^2\,dy_R}\hat{\sigma}(\gamma\gamma\to R), \tag{3.10}$$

[5] See also [13,120,154,157,159,187–208] for related issues.

where M_R and y_R are the mass and the rapidity of the resonance R, and $\hat{\sigma}(\gamma\gamma \to R)$ shows the parton-level cross section for the process $\gamma\gamma \to R$. The inclusive luminosity function can be conveniently written in terms of the photon PDF as

$$\frac{d\mathcal{L}^{\rm inc}_{\gamma\gamma}}{dM_R^2\, dy_R} = \frac{1}{s}\gamma(x_1,\mu)\,\gamma(x_2,\mu), \tag{3.11}$$

where $x_{1,2} = \frac{M_R}{\sqrt{s}}e^{\pm y_R}$ represent the momentum fractions of the photons inside the protons and $\sqrt{s}$ means the total energy. The value of $\gamma(x,\mu)$ can be evaluated by taking the Dokshitzer–Gribov–Lipatov–Altarelli–Parisi (DGLAP) evolution from the starting scale μ_0 (= 1 GeV) to μ after an estimation of coherent and incoherent components of the initial form of $\gamma(x,\mu=\mu_0)$ at $\mu=\mu_0$ (see [185] for details).

By adopting the narrow width approximation, which is fine in our case, the parton-level cross section of the particle S of mass m_S and rapidity y_S is

$$\begin{aligned}\hat{\sigma}(\gamma\gamma \to S) &= \frac{8\pi^2\Gamma(S\to\gamma\gamma)}{m_S}\delta(M_R^2 - m_S^2)\\ &= \frac{8\pi^2\Gamma_{\rm tot}(S)}{m_S}\mathcal{B}(S\to\gamma\gamma)\delta(M_R^2 - m_S^2).\end{aligned} \tag{3.12}$$

The inclusive differential cross section is obtained in a factorized form:

$$\frac{d\sigma^{\rm inc}(p(\gamma)p(\gamma)\to S+X)}{dy_S} = \frac{8\pi^2\Gamma(S\to\gamma\gamma)}{m_S}\times\left.\frac{d\mathcal{L}^{\rm inc}_{\gamma\gamma}}{dM_R^2\, dy_S}\right|_{M_R=m_S}. \tag{3.13}$$

Now taking the values for $\gamma(x,\mu)$ in Ref. [185], we obtain a convenient form of cross section

$$\sigma^{\rm inc}(p(\gamma)p(\gamma)\to S+X) = 91\ {\rm fb}\left(\frac{\Gamma_{\rm tot}(S)}{1\ {\rm GeV}}\right)\mathcal{B}(S\to\gamma\gamma) \tag{3.14}$$

or

$$\sigma^{\rm inc}(p(\gamma)p(\gamma)\to S+X\to\gamma\gamma+X) = 91\ {\rm fb}\left(\frac{\Gamma_{\rm tot}(S)}{1\ {\rm GeV}}\right)\mathcal{B}^2(S\to\gamma\gamma), \tag{3.15}$$

for evaluating production cross sections at $\sqrt{s} = 13$ TeV. The reference magnitude of the cross section, 91 fb, is much greater than that in Ref. [40] obtained under the narrow width approximation and effective photon approximation [209,210], 1.6–3.6 fb (depending on the minimum impact parameter for elastic scattering), while it is smaller than that in Ref. [188] through a similar calculation in Ref. [185], 240 fb. We also find at $M_R = 750$ GeV in Ref. [185],

$$\frac{\mathcal{L}^{\rm inc}_{\gamma\gamma}(\sqrt{s}=13\ {\rm TeV})}{\mathcal{L}^{\rm inc}_{\gamma\gamma}(\sqrt{s}=8\ {\rm TeV})} \approx 2.9. \tag{3.16}$$

Having the above relations in Eqs. (3.14)–(3.16), it is straightforward to evaluate the inclusive production cross section at $\sqrt{s} = 8$ TeV. We note that the resultant value is greater than the value (≈ 2) cited in Ref. [188].

Table 2. 95% C.L. upper bounds on decay channels of a 750 GeV scalar resonance.

Final state	Upper bound (in fb, 95% C.L.)	Category	Ref.
$\gamma\gamma$	2.4/2.4	8 TeV-ATLAS/CMS	[126,127]
	13/13	13 TeV-ATLAS/CMS	[3,4]
$Z\gamma$	4.0/27	8 TeV/13 TeV-ATLAS	[211,212]
ZZ	12/99	8 TeV/13 TeV-ATLAS	[130,213]
WW	35	8 TeV-ATLAS	[214]
hh	40	8 TeV-ATLAS	[215]

3.2. Results

3.2.1. Case 1: Without mass mixing

In this part, we discuss the case that the field S is a mass eigenstate, where no mixing effect is present through mass terms with other scalars. Under our assumptions, the relevant parameters are $(m_{k^{\pm\pm}}, \mu_{Sk}, N_j)$: the universal physical mass of the doubly charged scalars (assuming $m_{k^{\pm\pm}} = m_{j_a^{\pm\pm}}$ for all a), the universal effective scalar trilinear coupling (assuming $\mu_{Sk} = \mu_{Sj_a}$ for all a), and the number of additional doubly charged singlet scalars. We observe the unique relation among the branching ratios of S irrespective of $m_{k^{\pm\pm}}$ and μ_{Sk}, which is suggested by Eq. (3.1), as

$$\mathcal{B}(S \to \gamma\gamma) \simeq 0.591, \quad \mathcal{B}(S \to \gamma Z) \simeq 0.355, \quad \mathcal{B}(S \to ZZ) \simeq 0.0535. \tag{3.17}$$

In Ref. [216], reasonable target values for the cross section of $\sigma_{\gamma\gamma} \equiv \sigma(pp \to S + X \to \gamma\gamma + X)$ at the $\sqrt{s} = 13$ TeV Large Hadron Collider (LHC) were discussed as functions of the variable $R_{13/8}$, which is defined as

$$R_{13/8} \equiv \frac{\sigma(pp \to S)|_{\sqrt{s}=13\ \mathrm{TeV}}}{\sigma(pp \to S)|_{\sqrt{s}=8\ \mathrm{TeV}}}, \tag{3.18}$$

where the published data after Moriond 2016 are included, and the four categories distinguished by the two features (spin-0 or spin-2; narrow width $[\Gamma_S/m_S \to 0]$ or wide width $[\Gamma_S/m_S = 6\%]$) are individually investigated. As pointed out in Eq. (3.17), the value of $\mathcal{B}(S \to \gamma\gamma)$ is uniquely fixed as $\simeq 60\%$ and S is produced only through photon fusion in the present case. As shown in Eq. (3.16) in our estimation of the photo-production, $R_{13/8}$ corresponds to 2.9, where the best fit values of $\sigma_{\gamma\gamma}$ at $\sqrt{s} = 13$ TeV are extracted from [216] as

$$2.0 \pm 0.5\ \mathrm{fb} \quad (\text{for } \Gamma_S/m_S \to 0), \quad 4.25 \pm 1.0\ \mathrm{fb} \quad (\text{for } \Gamma_S/m_S = 6\%). \tag{3.19}$$

The theoretical error in the present formulation of the photo-production was evaluated as ± 15–20% in [185]. Then, we decide to focus on the 2σ favored regions including the error (20%, fixed) also, concretely speaking,

$$[0.8, 3.6]\ \mathrm{fb} \quad (\text{for } \Gamma_S/m_S \to 0), \quad [1.8, 7.5]\ \mathrm{fb} \quad (\text{for } \Gamma_S/m_S = 6\%). \tag{3.20}$$

Here, the 95% C.L. upper bound on $\sigma_{\gamma\gamma}$ at $\sqrt{s} = 8$ TeV is $\lesssim 2.4$ fb [126,127] and the favored regions are still consistent with the 8 TeV result (or just on the edge). It is found that the bounds on the $Z\gamma$, ZZ final states are weaker than that of $\gamma\gamma$. Relevant information is summarized in Table 2.

In Fig. 2, situations in our model are summarized. Six cases with different numbers of doubly charged scalars are considered with $N_j = 0$, 1, 10, 100, 200, and 300. Here, we should mention

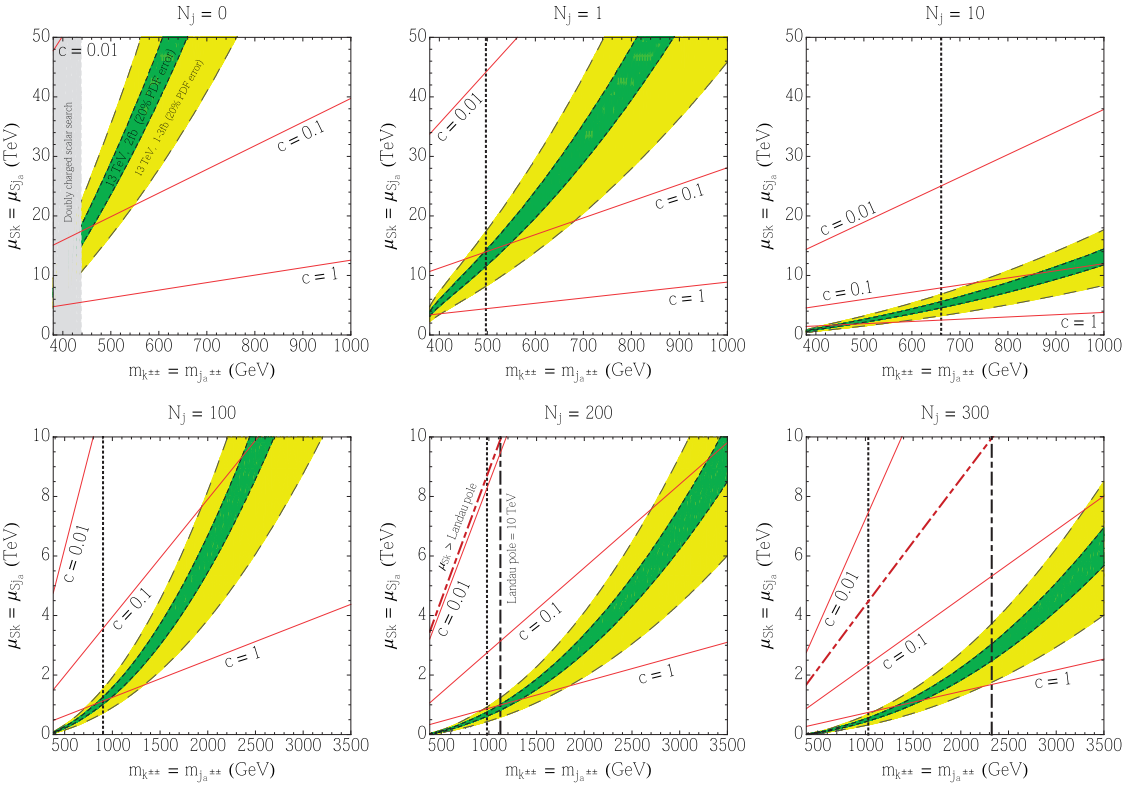

Fig. 2. Six cases with different numbers of doubly charged scalars are considered with $N_j = 0, 1, 10, 100, 200$, and 300. Inside the green regions, the best-fit value of the production cross section is realized by taking account of $\pm 20\%$ theoretical error discussed in Ref. [185]. The yellow regions indicate the areas where we obtain the 2σ-favored values in the production cross section of $p(\gamma)p(\gamma) \to S + X \to \gamma\gamma + X$, where we take account of both the theoretical ($\pm 20\%$) and experimental (shown in Eq. (3.19)) errors. Cross-section evaluations are due to Eq. (3.15). The gray shaded region $m_{k^{\pm\pm}} \leq 438$ GeV in $N_j = 0$ shows the excluded parts in the 95% C.L. via the ATLAS 8 TeV search for doubly charged particles with the assumption of $\mathcal{B}(k^{\pm\pm} \to \mu^\pm\mu^\pm) = 100\%$ [218]. The vertical black dotted lines represent corresponding bounds on the universal physical mass $m_{k^{\pm\pm}}$ when we assume $\mathcal{B}(j_a^{\pm\pm} \to \mu^\pm\mu^\pm) = 100\%$ for all $j_a^{\pm\pm}$. Two types of constraints with respect to the "Landau pole" of g_Y (defined as $g_Y(\mu) = 4\pi$) are meaningful when N_j is large ($N_j = 200, 300$). The red lines indicate three reference boundaries of the correction factor $c\,\delta = 1$ with $c = 1, 0.1, 0.01$ to the trilinear couplings μ_{Sk} ($= \mu_{Sj_a}$) defined in Eq. (3.22). For each choice of c, the region below the corresponding boundary is favored from the viewpoint of perturbativity.

an important issue. As indicated in Fig. 2, when N_j is zero, more than $10 \sim 20$ TeV is required in the effective trilinear coupling μ_{Sk}. Such a large trilinear coupling would immediately lead to a violation of tree-level unitarity in the scattering amplitudes including μ_{Sk}, e.g., $k^{++}k^{--} \to k^{++}k^{--}$ or $SS \to k^{++}k^{--}$ at around the energy 1 TeV, where the physics of our interest is spread. Also, the vacuum is possibly threatened by destabilization via the large trilinear coupling, which calls charge breaking minima. To avoid the problems, naively speaking, the value of μ_{Sk} is less than $1 \sim 5$ TeV.[6]

Also, we consider the doubly charged singlet scalars produced via $pp \to \gamma^*/Z + X \to k^{++}k^{--} + X$. Lower bounds at 95% C.L. on $m_{k^{\pm\pm}}$ via the 8 TeV LHC data were provided by the ATLAS group in Ref. [218] as 374 GeV, 402 GeV, 438 GeV when assuming a 100% branching ratio to $e^\pm e^\pm$,

[6] In the case of Minimal Supersymmetric Standard Model with a light $\tilde{t}_1$ (100 GeV), $A = A_t = A_b$, $\tan\beta \gg 1$, $m_A \gg M_Z$, $|\mu| \ll M_{\tilde{Q}}$ and $M_{\tilde{b}}$, the bound on the trilinear coupling $|A| \lesssim 5$ TeV was reported in Ref. [217].

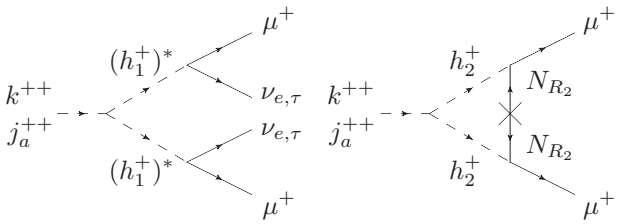

Fig. 3. A schematic description for the decay patterns of k^{++} or j_a^{++} with two anti-muons in the final state. Here, h_1^+'s in the left diagram are off-shell particles.

$e^\pm\mu^\pm$, $\mu^\pm\mu^\pm$ pairs, respectively. In our model, the doubly charged scalars can decay through the processes as shown in Fig. 3, where h_1^+'s are off shell since it should be heavy, at least 3 TeV. In the case of k^{++} in $N_j = 0$, when the values of μ_{11} and μ_{22} are the same or similar, from Eq. (2.2), the relative branching ratios between $k^{++} \to \mu^+\mu^+\nu_i\nu_j$ and $k^{++} \to \mu^+\mu^+$ are roughly proportional to $(y_L)_{2i}(y_L)_{2j}$ and $((y_R)_{22})^2$. As concluded in our previous work [150], the absolute value of $(y_R)_{22}$ should be as large as around $8 \sim 9$ to generate the observed neutrino properties, while a typical magnitude of $(y_L)_{2i}$ is $0.5 \sim 1$. Then, the decay branch $k^{++} \to \mu^+\mu^+$ is probably as dominant as $\sim 100\%$ and we need to consider the 8 TeV bound seriously. The simplest attitude would be to avoid examining the shaded regions in Fig. 2, which indicate the excluded parts in the 95% C.L. via the ATLAS 8 TeV data with the assumption of $\mathcal{B}(k^{\pm\pm} \to \mu^\pm\mu^\pm) = 100\%$ [218].

When one more doubly charged scalar j_1^{++} ($N_j = 1$) exists, a detailed analysis is needed for precise bounds on $k^{\pm\pm}$ and $j_1^{\pm\pm}$. Benchmark values are given in Fig. 2 by the vertical black dotted lines, which represent corresponding bounds on the universal physical mass $m_{k^{\pm\pm}}$ when we assume $\mathcal{B}(j_a^{\pm\pm} \to \mu^\pm\mu^\pm) = 100\%$ for all $j_a^{\pm\pm}$. We obtain the 95% C.L. lower bounds on the universal mass value $m_{k^{\pm\pm}}$ as ~ 500 GeV ($N_j = 1$), ~ 660 GeV ($N_j = 10$), ~ 900 GeV ($N_j = 100$), ~ 980 GeV ($N_j = 200$), and ~ 1030 GeV ($N_j = 300$), respectively, through numerical simulations by `MadGraph5_aMC@NLO` [219,220] with the help of `FeynRules` [221–223] for model implementation.

The method that we adopt for evaluating the corresponding 95% C.L. bounds with the assumption of $\mathcal{B}(j_a^{\pm\pm} \to \mu^\pm\mu^\pm) = 100\%$ for all $j_a^{\pm\pm}$, where more than one doubly charged scalar exists, is as follows. When N doubly charged scalars are present, the expected number of the total signal receives the multiplicative factor N. Following this statement, we can estimate the bound on the universal mass $m_{k^{\pm\pm}}$ via the pair production cross section of a doubly charged scalar $k^{\pm\pm}$ (in the $N = 1$ case) through the sequence $pp \to \gamma^*/Z + X \to k^{++}k^{--} + X$. The bound should correspond to the mass where the production cross section is N times smaller than the benchmark value in $m_{k^{\pm\pm}} = 438$ GeV, which is the 95% C.L. lower bound on $m_{k^{\pm\pm}}$ from the ATLAS 8 TeV data [218]. We obtained the leading-order cross section as 0.327 `fb`, which is fairly close to the ATLAS value, 0.357 `fb` read from Fig. 4(c) of Ref. [218]. In calculations, we used the `CTEQ6L` proton PDF [224] and set the renormalization and factorization scales to $2m_{k^{\pm\pm}}$.

Here, we point out an interesting possibility. From Eq. (2.9), if $\lambda_{11}^{(1)}\langle\Sigma_0^*\rangle$ is rather larger than $\mu_{22}^{(1)}$, the pattern $j_1^{++} \to \mu^+\mu^+\nu_i\nu_j$ possibly becomes considerable, where we cannot reconstruct the invariant mass of the doubly charged scalar since missing energy exists in this decay sequence. Then, the significance for exclusion would be dropped and we could relax the bound on $m_{j_1^{\pm\pm}}$ to some extent. An extreme case is with a nonzero $\lambda_{11}^{(1)}\langle\Sigma_0^*\rangle$ and $\mu_{22}^{(1)} = 0$, where the branching ratio of $j_1^{++} \to \mu^+\mu^+$ becomes zero at the one-loop level and the significance takes the lowest value, which

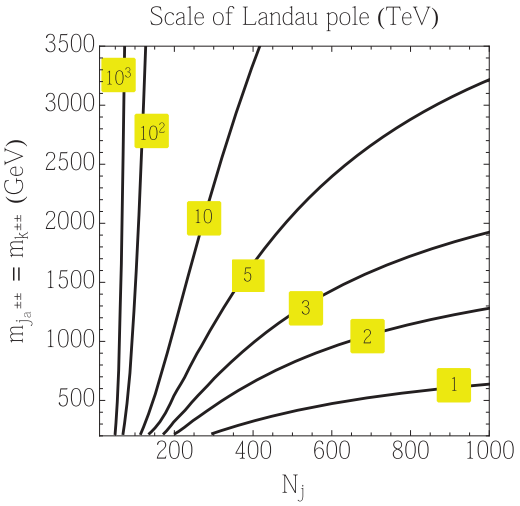

Fig. 4. Positions of the "Landau pole" defined as $g_{\rm Y}(\mu) = 4\pi$.

is the best for avoiding the 8 TeV LHC bound. Also in this situation, no additional contribution to the neutrino mass matrix exists and the original successful structure is not destroyed. Similar discussions are applicable when N_j is more than 1.

When we assume 100% branching fractions in $j_a^{++} \to \mu^+\mu^+$ for all j_a^{++}, the common trilinear coupling μ_{Sk} should be larger than $\sim$ 10 TeV ($N_j = 0$), $\sim$ 8 TeV ($N_j = 1$), $\sim$ 3 TeV ($N_j = 10$), less than 1 TeV ($N_j = 100$, 200, 300), to obtain a reasonable amount of the production cross section taking into account the $\pm 20\%$ theoretical error in cross section as suggested by Fig. 2. As mentioned, large trilinear couplings $\lambda_{11}^{(a)}\langle\Sigma_0^*\rangle$ can help us to alleviate the 8 TeV bound.

Another theoretical bound is reasonably expected when, as in the present situation, many new particles with nonzero gauge charges are introduced around 1 TeV. The presence of multiple doubly charged $\mathrm{SU}(2)_L$ singlet scalars deforms the energy evolution of the $U(1)_{\rm Y}$ gauge coupling $g_{\rm Y}$ as

$$\frac{1}{g_{\rm Y}^2(\mu)} = \frac{1}{g_{\rm Y}^2(m_{\rm input})} - \frac{b_{\rm Y}^{\rm SM}}{16\pi^2}\log\left(\frac{\mu^2}{m_{\rm input}^2}\right) - \theta(\mu - m_{\rm threshold})\frac{\Delta b_{\rm Y}}{16\pi^2}\log\left(\frac{\mu^2}{m_{\rm threshold}^2}\right), \quad (3.21)$$

where $b_{\rm Y}^{\rm SM} = 41/6$, $\Delta b_{\rm Y} = 4/3(N_j + 1)$, and we implicitly assume the relation $m_{\rm input}$ $(= m_Z) < m_{\rm threshold}$ $(= m_{k^{\pm\pm}} = m_{j_a^{\pm\pm}})$. As a reasonable criterion, we require that the theory is still not drastically strongly coupled within the LHC reach $\sim$ 10 TeV.[7] Positions of the "Landau pole" μ, which is defined as $g_{\rm Y}(\mu) = 4\pi$, are calculated with ease as functions of N_j and $m_{\rm threshold}$ $(= m_{k^{\pm\pm}} = m_{j_a^{\pm\pm}})$ as shown in Fig. 4. Now, we recognize that under the criterion, the case with $N_j \lesssim 100$ is not restricted in the sense that the bound via the "Landau pole" is much weaker than the phenomenological requirement $m_{k^{\pm\pm}}$ $(= m_{j_a^{\pm\pm}}) \gtrsim 375$ GeV (for preventing the decays $S \to k^{++}k^{--}, j_a^{++}j_a^{--}$). On the other hand when N_j is rather larger than 100, meaningful bounds are expected from Fig. 4. For example, when $N_j = 200$ (300), $m_{k^{\pm\pm}}$ $(= m_{j_a^{\pm\pm}})$ should be greater than $\sim$ 1.1 TeV ($\sim$ 2.2 TeV).

[7] We note that measurements of running electroweak couplings put bounds on additional contributions to the beta functions of the $\mathrm{SU}(2)_L$ and $U(1)_{\rm Y}$ gauge couplings [225] even though the work [225] did not survey the parameter range that is relevant to our discussion. Similar discussions have been had in the quantum chromodynamics (QCD) coupling [226,227], which is basically irrelevant in our case.

There also arises a largish loop contribution to the universal trilinear coupling μ_{Sk} ($= \mu_{Sj_a}$) as

$$\mu_{Sk} \to \mu_{Sk}\,(1 + c\,\delta), \quad \delta = \frac{N_j + 1}{16\pi^2} \times \left(\frac{\mu_{Sk}}{m_{k^{\pm\pm}}}\right)^2. \tag{3.22}$$

A convenient parameter, $c \lesssim 1$, encapsulates the effects from all higher-order contributions. Precise determination of c is beyond the scope of this paper thus, instead, we show the cases with $c = 0.01$, 0.1, and 1 as benchmarks (see Fig. 2). It is easily noticed that the loop-induced value could dominate over the tree-level value unless $c\,\delta < 1$, or equivalently $\mu_{Sk}/m_{k^{\pm\pm}} < 4\pi/[c(N_j + 1)]^{1/2}$. This may affect the convergence of the multiloop expansion even though the theory is still renormalizable.[8]

Unfortunately when N_j is only a few, explaining the diphoton excess is not consistent since the value of μ_{Sk} is too large and tree-level unitarity is violated. This problem is avoided when $N_j \gtrsim 10$, whereas the evolution of g_Y through the renormalization group effect puts additional bounds on $m_{k^{\pm\pm}}$ ($= m_{j_a^{\pm\pm}}$) when $N_j \gtrsim 100$. The preferred parameter would be further constrained by $c\,\delta < 1$ as in Fig. 2. In conclusion, we can explain the 750 GeV excess consistently even when $\mathcal{B}(j_a^{\pm\pm} \to \mu^\pm\mu^\pm) = 100\%$ for all $j_a^{\pm\pm}$.

3.2.2. Case 2: With mass mixing

In this section, we investigate the situation when the mass mixing between S and Φ are allowed. At first, we phenomenologically introduce the mixing angle β as

$$\begin{pmatrix}\phi\\ S\end{pmatrix} = \begin{pmatrix}c_\beta & s_\beta\\ -s_\beta & c_\beta\end{pmatrix}\begin{pmatrix}h\\ S'\end{pmatrix}, \tag{3.23}$$

where we use the shorthand notation $c_\beta \equiv \cos\beta$, $s_\beta \equiv \sin\beta$, and express the observed 125 GeV and 750 GeV scalars (mass eigenstates) by h and S', respectively. We assume the following effective interactions among scalars:

$$\Delta\mathcal{V}_{\rm eff} = \tfrac{1}{2}m_h^2h^2 + \tfrac{1}{2}m_{S'}^2S'^2 + \mu_{Sk}S|k^{++}|^2 + \mu_{Sj_a}S|j_a^{++}|^2 + \hat{\mu}_{S\Phi}S|\Phi|^2 + \hat{\lambda}_{S\Phi}S^2|\Phi|^2, \tag{3.24}$$

where m_h and $m_{S'}$ represent the mass eigenvalues 125 GeV and 750 GeV; μ_{Sk} and μ_{Sj_a} are effective trilinear couplings as defined in Eq. (2.10), where the contents of them are not important in this study. We note that we safely ignore the terms $\phi|k^{++}|^2$ and $\phi|j_a^{++}|^2$ since these terms originate from the gauge-invariant interactions $|\Phi|^2|k^{++}|^2$ and $|\Phi|^2|j_a^{++}|^2$, where effective trilinear couplings of them are small compared with μ_{Sk} and μ_{Sj_a}. Because of the mixing in Eq. (3.23), the terms $h|k^{++}|$ and $h|j_a^{++}|$ are induced and can affect the signal strength of h.

The S'-h-h interaction may be also introduced via the interaction Lagrangian:

$$\tfrac{1}{2}\mu_{S'h}S'h^2 \quad \text{with} \quad \mu_{S'h} \equiv m_{S'h}\left[c_\beta^3 - 2c_\beta s_\beta^2\right], \tag{3.25}$$

where $m_{S'h}$ represents a mass scale and the mixing factor could be determined via the gauge-invariant term $S|\Phi|^2$. When $\langle S\rangle = 0$, the scale of $m_{S'h}$ is determined through the two mass eigenvalues and

[8] One should note, however, that $c\,\delta < 1$ is not an absolute requirement for a consistent theory. See, e.g., Ref. [228] where a loop-induced value overwhelms the tree-level counterpart in the context of the two Higgs doublet model.

the mixing angle β as

$$m_{S'h} = \left(\frac{m_{S'}^2 - m_h^2}{v}\right)\sin(2\beta), \tag{3.26}$$

since the mass mixing term $S\phi$ and the three point vertex $S\phi^2$ have the unique common origin $S|\Phi|^2$. Plots in this situation are provided in Appendix C.

A significant distinction from the previous no-mixing case is that the 750 GeV scalar can couple to the SM particles through the mixing effect. The inclusive production cross section at the LHC is deformed as

$$\sigma(pp \to S' + X) \simeq (\sigma^{\rm ggF}_{pp\to H^{\rm SM}_{750\,\rm GeV}} + \sigma^{\rm VBF}_{pp\to H^{\rm SM}_{750\,\rm GeV}})s_\beta^2 + \sigma^{\rm pf}_{pp\to S'}, \tag{3.27}$$

where $\sigma^{\rm ggF}_{pp\to H^{\rm SM}_{750\,\rm GeV}}$ and $\sigma^{\rm VBF}_{pp\to H^{\rm SM}_{750\,\rm GeV}}$ represent the inclusive production cross section of the SM-like Higgs boson with 750 GeV mass through the gluon fusion and vector boson fusion processes, respectively, and $\sigma^{\rm pf}_{pp\to S'}$ shows a corresponding value through the photon fusion in Eq. (3.14). We adopt the following digits in [91,129,229,230]:

$$\sigma^{\rm ggF}_{pp\to H^{\rm SM}_{750\,\rm GeV}} = \begin{cases} 156.8\,\text{fb} & \text{at } \sqrt{s} = 8\ \text{TeV}, \\ 590\,\text{fb} & \text{at } \sqrt{s} = 13\ \text{TeV}, \end{cases} \quad \sigma^{\rm VBF}_{pp\to H^{\rm SM}_{750\,\rm GeV}} = \begin{cases} 50\,\text{fb} & \text{at } \sqrt{s} = 8\ \text{TeV}, \\ 220\,\text{fb} & \text{at } \sqrt{s} = 13\ \text{TeV}, \end{cases} \tag{3.28}$$

$$\Gamma_{\rm tot}(H^{\rm SM}_{750\,\rm GeV}) = 247\ \text{GeV}, \quad \mathcal{B}(H^{\rm SM}_{750\,\rm GeV} \to WW) = 58.6\%, \quad \mathcal{B}(H^{\rm SM}_{750\,\rm GeV} \to ZZ) = 29.0\%. \tag{3.29}$$

Part of the relevant partial decay widths are written down as

$$\Gamma_{S'\to WW} = \Gamma_{H^{\rm SM}_{750\,\rm GeV}\to WW}\, s_\beta^2, \tag{3.30}$$

$$\Gamma_{S'\to hh} \sim \frac{(\mu_{S'h})^2}{32\pi m_{S'}}\left(1 - \frac{4m_h^2}{m_{S'}^2}\right)^{1/2}, \tag{3.31}$$

and the total width takes the form

$$\Gamma_{\rm tot}(S') \sim \left[\Gamma_{\rm tot}(H^{\rm SM}_{750\,\rm GeV}) - \Gamma_{H^{\rm SM}_{750\,\rm GeV}\to ZZ}\right]s_\beta^2 + \Gamma_{S'\to\gamma\gamma} + \Gamma_{S'\to Z\gamma} + \Gamma_{S'\to ZZ} + \Gamma_{S'\to hh}, \tag{3.32}$$

where the minuscule parts $\mathcal{B}(H^{\rm SM}_{750\,\rm GeV} \to \gamma\gamma) = 1.79 \times 10^{-5}\%$, $\mathcal{B}(H^{\rm SM}_{750\,\rm GeV} \to Z\gamma) = 1.69 \times 10^{-4}\%$, and $\mathcal{B}(H^{\rm SM}_{750\,\rm GeV} \to gg) = 2.55 \times 10^{-2}\%$ [129] could be safely neglected. Here, $\Gamma_{S'\to\gamma\gamma}$, $\Gamma_{S'\to Z\gamma}$, and $\Gamma_{S'\to ZZ}$ describe decay widths at the one-loop level, where the multiple doubly charged scalars propagate in the loops. When we take the limit $s_\beta \to 0$, they are reduced to Eqs. (3.2)–(3.4). Explicit forms of these widths are summarized in Appendix B.

In Fig. 5, prospects are widely discussed in the choice of the mass of the degenerate doubly charged scalars ($m_{k^{\pm\pm}}\,[= m_{j_a^{\pm\pm}}] = 900$ GeV) and two different choices of $m_{S'h}$ (0.5 TeV [left panel] and 1.9 TeV [right panel]). First, we emphasize that the 125 GeV Higgs h couples to the doubly charged scalars through the mixing in Eq. (3.23) in the present setup. As in Ref. [150], we take the results at $\sqrt{s} = 7$ and 8 TeV of the five Higgs decay channels reported by the ATLAS and CMS experiments into consideration, which are $h \to \gamma\gamma$, $h \to ZZ$, $h \to WW$, $h \to b\bar{b}$, $h \to \tau^+\tau^-$ [231–236], and

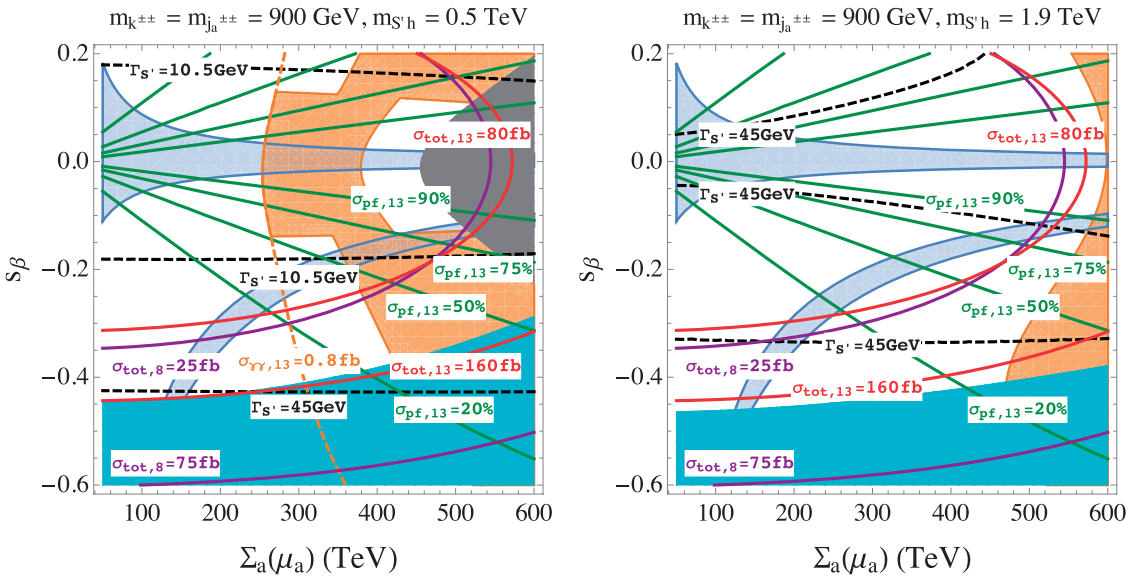

Fig. 5. Allowed ranges of the parameters $\{\Sigma_a(\mu_a), s_\beta\}$ are shown in the choice of the mass of the degenerate doubly charged scalars ($m_{k^{\pm\pm}}$ [$= m_{j_a^{\pm\pm}}$] $= 900$ GeV) and two different choices of $m_{S'h}$ (0.5 TeV [left panel] and 1.9 TeV [right panel]). The light blue regions represent 2σ allowed regions of 125 GeV Higgs signal strengths, while the orange regions suggest the areas where the 750 GeV excess is suitably explained. The gray/cyan regions are excluded in 95% C.L.s by the ATLAS 8 TeV results for $S' \to \gamma\gamma/ZZ$. For better understanding, several contours for the total width of S' ($\Gamma_{S'}$), total production cross sections at $\sqrt{s} = 8/13$ TeV ($\sigma_{\mathrm{tot},8/13}$), and the percentage of the production through the photon fusion at $\sqrt{s} = 13$ TeV ($\sigma_{\mathrm{pf},13}$) are illustrated.

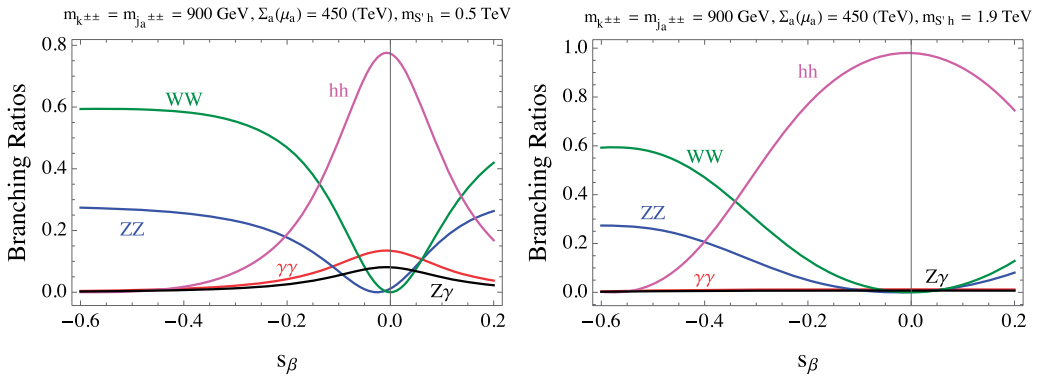

Fig. 6. Relevant branching ratios of S' in the two configurations in Fig. 5 are shown. Here, values of $\Sigma_a(\mu_a)$ are suitably fixed as typical digits in the corresponding allowed regions.

calculate a χ^2 variable for estimating 2σ allowed ranges of the parameter space, which are depicted in light blue.[9] Here, we find two types of allowed regions with and without including $s_\beta = 0$, which correspond to the cases with and without accidental cancelation between SM contributions and the new contributions through the mixing, respectively.

The orange regions suggest the 2σ-favored areas with taking account of the 20% theoretical error in the present way for photon-fusion production cross section summarized in Eq. (3.20). Here, for

[9] The original model contains invisible channels in the 125 GeV Higgs boson due to the existence of a dark matter candidate and a Nambu–Goldstone boson from the spontaneous breaking of a global $U(1)$. We ignore the invisible widths in the global fit for simplicity.

an illustration we use the values in the cases of $\Gamma/m \to 0$ and $\Gamma/m = 6\%$ for the regions $\Gamma/m < 1\%$ and $\Gamma/m \geq 1\%$, respectively. The gray/cyan regions are excluded in 95% C.L.s by the ATLAS 8 TeV results for $S' \to \gamma\gamma/ZZ$. For a better understanding, several contours for the total width of S' ($\Gamma_{S'}$), total production cross sections at $\sqrt{s} = 8/13$ TeV ($\sigma_{\text{tot},8/13}$), and the percentage of the production through the photon fusion at $\sqrt{s} = 13$ TeV ($\sigma_{\text{pf},13}$) are illustrated. Relevant branching ratios of S' are shown in Fig. 6 for the two configurations in Fig. 5.

Now we focus on two types of consistent solutions around $s_\beta \simeq 0$ and $s_\beta \simeq -0.15$. The physics in the situation $s_\beta \simeq 0$ is basically the same as the previous "case 1" without the mass mixing effect, where the total decay width is small, concretely less than 1 GeV. On the other hand, when $s_\beta \simeq -0.15$, partial widths of decay branches that are opened by a nonzero value of s_β become sizable and expected values of the total width can become, interestingly, near 10.5 GeV or 45 GeV, which are the latest 13 TeV best-fit values of the CMS and ATLAS groups, respectively.

Finally, we briefly comment on tree-level unitarity. When we consider $m_{k^{\pm\pm}}$ [$= m_{j_a^{\pm\pm}}$] = 900 GeV, the bound via tree-level unitarity is relaxed in both $s_\beta \simeq 0$ and $s_\beta \simeq -0.15$. However, with a large value of the universal trilinear coupling in the 3 to 6 TeV range, $c\,\delta < 1$ is achieved only if $c \ll 1$ when $\mathcal{B}(j_a^{\pm\pm} \to \mu^\pm\mu^\pm) = 100\%$ for all $j_a^{\pm\pm}$, which may require further model-building efforts.

4. Conclusion and discussion

In this paper, we investigated a possibility for explaining the recently announced 750 GeV diphoton excess by the ATLAS and CMS experiments at the CERN LHC in the context of loop-induced singlet production and decay through photon fusion. When a singlet scalar S, which is a candidate of the resonance particle, couples to doubly charged particles, we can obtain a suitable amount of the cross section of $pp \to S + X \to \gamma\gamma + X$ without introducing a tree-level production of S. In three-loop radiative neutrino models, $\text{SU}(2)_L$ singlet multiple doubly charged scalars are introduced such that the S-γ-γ vertex is radiatively generated and enhanced. When we consider such doubly charged scalar(s), the branching ratio $\mathcal{B}(S \to \gamma\gamma)$ is uniquely fixed at $\simeq 60\%$ by quantum numbers when S is a mass eigenstate. Constraints from 8 TeV LHC data are all satisfied.

A fascinating feature in the single S production through photon fusion is that the value of $\mathcal{B}(S \to \gamma\gamma)$ as well as Γ_S determines the production cross section, as shown in Eqs. (3.14) and (3.15). With the branching fraction to diphoton $S \to \gamma\gamma \simeq 60\%$ (see Sect. 3.2.1), when we take the "wide-width" scenario with $\Gamma/m \sim 6\%$, the expected cross section to diphoton is too large. However, in the "narrow-width" scenario with $\Gamma_S = 62.9$ MeV, it fits nicely to the best-fit value for the inclusive cross section of 2 fb. We also note that the width is close to the $8 + 13$ TeV best-fit value announced by the CMS group (105 MeV) (see Appendix C). This is an informative prediction of our present scenario that should be tested in the near future. Also the relative strengths of the one-loop-induced partial decay widths are insensitive to N_j as shown in Eq. (3.1) when the mixing effect between S and the Higgs doublet Φ is negligible. This universality is a remarkable property of our scenario and this relation can be tested when more data is available.

When S and the Higgs doublet Φ can mix, some distinctive and interesting features are found. In the first thought, only a small mixing $\sin\beta \ll 1$ is allowed to circumvent drastic modifications to 125 GeV Higgs signal strengths but we can see another interesting region of parameter space with $\sin\beta \simeq -0.15$, where the 750 GeV excess can be explained consistently within the "wide-width" scenario (see Sect. 3.2.2). However a big part of the parameter space, especially in the

case with the scalar mixing, would lie outside the $c\,\delta < 1$ region, which requires $c \ll 1$ for a viable model.

Finally, we discuss further extensions of the model and other phenomenological issues.

- A possible extension of the present direction is to introduce N_S $SU(2)_L$ singlet scalars, ($S = S_1, S_2, \ldots, S_{N_S}$), without hypercharge in the theory. If the masses of the scalars are almost degenerate to 750 GeV, the current experiment may not be able to detect the multiple bumps so that they would look like a single bump as we see it. The total cross section, then, is enhanced by the multiplicative factor N_S^2 as

$$\sigma_{\rm tot}(pp \to \gamma\gamma + X) \approx N_S^2 \sigma(pp \to S + X \to \gamma\gamma + X). \tag{4.1}$$

- Another possible extension is that we also introduce the singly charged scalars $\tilde{h}^\pm_{1,2}$ that hold the same quantum numbers as $h^\pm_{1,2}$ and have the same interaction with $j_a^{\pm\pm}$ as $h^\pm_{1,2}$ do with $k^{\pm\pm}$. In such a possibility, contributions to the neutrino mass matrix are enhanced and we can reduce the value of the large coupling required for a consistent explanation in the original model, especially in $(y_R)_{22}$. See the appendix A for details.
- The triple coupling of the Higgs boson could be enhanced in our case that may activate strong first-order phase transition, which is a necessity for realizing the electroweak baryogenesis scenario [237]. In such a case, radiative seesaw models can explain not only neutrino mass and dark matter but also baryon asymmetry of the universe.
- The decays $k^{\pm\pm} \to \ell^\pm\ell^\pm$ and $j_a^{\pm\pm} \to \ell^\pm\ell^\pm$ provide very clean signatures. The 13 TeV LHC would be expected to replace the current bound on the universal mass, e.g., $m_{k^{\pm\pm}} > 438$ GeV when $\mathcal{B}(k^\pm/j_a^\pm \to \mu^\pm\mu^\pm) = 100\%$ for all the doubly charged scalars, from the 8 TeV data [218] soon. An important feature recognized from Fig. 2 is that when N_j is not so large as around 10, only light doubly charged scalars are consistent with the bound from tree-level unitarity. Such possibilities will be exhaustively surveyed and eventually confirmed or excluded in the near future. On the other hand, when N_j is as large as around 10, from Fig. 2, more than ~ 700 GeV doubly charged scalars can exist holding tree-level unitarity. Such heavy particles require a suitable amount of integrated luminosity for being tested in colliders. In other words, such possibilities will be hard to discard in the near future.
- It might be worth mentioning the distinction between our model discussed here and the other well-known radiative models, namely, the Zee model [131] at the one-loop level, the Zee–Babu model [133,134] at the two-loop level, the Kraus–Nasri–Trodden (KNT) model [136], the Aoki–Kanemura–Seto (AKS) model [137,138], and the Gustafsson–No–Rivera (GNR) model [139] at the three-loop level. Essentially, any model that includes isospin singlet charged bosons potentially explains the 750 GeV diphoton excess along the same lines as discussed in this paper. Among those, three-loop models have natural DM candidates by construction, which we regard as a phenomenologically big advantage. Our model shares this virtue. On the other hand, in view of the charged boson, our model and also the GNR model include doubly charged particles. From the currently available data, it is not possible to distinguish the effect of a singly charged scalar from a doubly charged scalar. However, we still see that a doubly charged boson is in favor of the explanation of the 750 GeV diphoton excess simply because of the enhanced diphoton coupling.

- As we discussed before, $k^{\pm\pm}$ decays to $\mu^\pm\mu^\pm$ with an almost 100% branching fraction, distinctively from other models, e.g., the Zee–Babu model, due to the large coupling $(y_R)_{22} \gtrsim 2\pi$, which is required to realize the observed neutrino data in our setup consistently.

Note Added: In the recent update in ICHEP 2016 (on 5th August 2016) after we submitted this manuscript to PTEP, which includes the analyzed data accumulated in 2016 (ATLAS: 15.4 fb^{-1}, CMS: 12.9 fb^{-1}), the 750 GeV diphoton signal now turns out to be statistically disfavored [238,239]. Nevertheless, we are still motivated to study the diboson resonance which may show up in a higher energy domain[10] and the generic results in this paper would be useful in the future in any case.

Acknowledgements

S.K., K.N., Y.O., and S.C.P. thank the workshop, Yangpyung School 2015, for providing us with an opportunity to initiate this collaboration. We are grateful to Eung Jin Chun, Satoshi Iso, Takaaki Nomura, and Hiroshi Yokoya for fruitful discussions. K.N. thanks Koichi Hamaguchi for useful comments when the first revision had been prepared. S.K. was supported in part by Grant-in-Aid for Scientific Research, Ministry of Education, Culture, Sports, Science and Technology (MEXT), No. 23104006, and Grant H2020-MSCA-RISE- 2014 No. 645722 (Non-minimal Higgs). This work is supported in part by the National Research Foundation of Korea (NRF) Research No. 2009-0083526 (Y.O.) of the Republic of Korea. S.C.P. is supported by an NRF grant funded by the Korean government (MSIP) (Nos. 2016R1A2B2016112 and 2013R1A1A2064120). This work was supported by IBS under the project code IBS-R018-D1 for R.W.

Funding

Open Access funding: SCOAP[3].

Appendix A. Brief review of the original model

Here, we briefly summarize features in the model discussed in Ref. [150].

(a) In this model, the sub-eV neutrino masses are radiatively generated at the three-loop level with the loop suppression factor $1/(4\pi)^6$. In such a situation, a part of couplings, including scalar trilinear couplings, contributing to the neutrino matrix tends to be close to unity.
(b) When a scalar trilinear coupling is large, it can put a negative effect on scalar quartic couplings at the one-loop level, which threatens the stability of the vacuum.
(c) The doubly charged scalar $k^{\pm\pm}$ is isolated from the charged lepton at the leading order under the assignment of the global $U(1)$ charges summarized in Table 1. Then, the charged particle does not contribute to lepton-flavor-violating processes significantly and a few hundred GeV mass is possible.
(d) The two singly charged scalars $h_1^\pm$ and $h_2^\pm$ have couplings to the charged leptons at the tree level. Since in our model a part of couplings are sizable, constraints from lepton flavor violations and vacuum stability do not allow a few hundred GeV masses, especially when $k^{\pm\pm}$ is around a few hundred GeV. The result of the global analysis in our previous paper [150] says that when $k^{\pm\pm}$ is 250 GeV (which is around the minimum value of $m_{k^{\pm\pm}}$), $m_{h_1^\pm}$ and $m_{h_2^\pm}$ should be greater than 3 TeV.
(e) In the allowed parameter configurations, we found that the absolute value of the coupling $(y_R)_{22}$ (in front of $\bar{N}_{R_2} e^c_{R_2} h_2^-$) tends to be $8 \sim 9$, while the peak of the distribution of the scalar trilinear

[10] It is suggested that additional jet activity could provide a useful handle to understand the underlying physics of heavy resonance in Ref. [240].

couplings $\mu_{11} \equiv \lambda_{11} v'/\sqrt{2}$ (in front of $h_1^- h_1^- k^{++}$) and μ_{22} (in front of $h_2^+ h_2^+ k^{--}$) is around $14 \sim 15$ TeV. We assumed that values of μ_{11} and μ_{22} are the same and real in the analysis.

(f) The two *CP* even components are mixed each other as shown in Eq. (2.4). By the (simplified) global analysis in Ref. [150] based on the data in Refs. [231–236], the sine of the mixing angle α should be

$$|\sin\alpha| \lesssim 0.3, \tag{A.1}$$

within 2σ allowed regions.

(g) On the other hand, the observed relic density requires a specific range of $\sin\alpha$. In our model, the Majorana DM N_{R_1} communicates with the SM particles and the $U(1)$ NG boson G through the two *CP* even scalars h and H. When v' is $\mathcal{O}(1)$ TeV, DM – DM – h/H couplings are significantly suppressed as (M_{N_1}/v') and then we should rely on the two scalar resonant regions. When we consider the situation $m_{\rm DM}/2 \simeq m_h$ ($\simeq 125$ GeV), a reasonable amount of the mixing angle α is required as

$$|\sin\alpha| \gtrsim 0.3, \tag{A.2}$$

where a tense situation with Eq. (A.1) is observed. The allowed range of v' is a function of $\sin\alpha$ and the maximum value is

$$v'|_{\rm max} \sim 9 \text{ TeV when } |\sin\alpha| \sim 0.3. \tag{A.3}$$

When the other resonant point is selected as $m_{\rm DM}/2 \simeq m_H$, the requirement on the angle is

$$|\sin\alpha| \lesssim 0.3 \tag{A.4}$$

when $m_H = 250$ GeV or a bit more. We find that the heavy H as $m_H = 500$ GeV cannot explain the relic density because of the suppression in the resonant propagator of H. The maximum of v' is found as

$$v'|_{\rm max} \sim 6 \text{ TeV when } 0 \lesssim |\sin\alpha| \lesssim 0.05, \tag{A.5}$$

where the couplings of H to the SM particles become so weak and hard to be excluded from the 8 TeV LHC results.

Appendix B. Decay widths at one loop

Here, we summarize the forms of relevant decay widths at the one-loop level in the presence of the scalar mixing in Eq. (3.23). We mention that we ignore $\Gamma_{S'\to gg}$ since this value is tiny because of the fact $\mathcal{B}(H^{\rm SM}_{750\,\rm GeV} \to gg) = 2.55 \times 10^{-2}\%$. The widths of the 125 GeV Higgs boson are used for global fits of signal strengths of the observed Higgs:

$$\Gamma_{h\to gg} = \frac{\alpha_s^2 m_h^3}{72\pi^3 v^2} \left| \frac{3}{4} \left(A_{1/2}^{\gamma\gamma}(\tau_t^{\rm SM}) \right) c_\beta \right|^2, \tag{B.1}$$

$$\Gamma_{h\to\gamma\gamma} = \frac{\alpha_{\rm EM}^2 m_h^3}{256\pi^3 v^2} \left| \left(A_1^{\gamma\gamma}(\tau_{\rm W}^{\rm SM}) + N_C Q_t^2 A_{1/2}^{\gamma\gamma}(\tau_t^{\rm SM}) \right) c_\beta + \frac{1}{2} \frac{v[\Sigma_a \mu_a]}{m_{k^{\pm\pm}}^2} Q_k^2 A_0^{\gamma\gamma}(\tau_k^{\rm SM})(-s_\beta) \right|^2, \tag{B.2}$$

$$\Gamma_{h\to Z\gamma} = \frac{\alpha_{\rm EM}^2 m_h^3}{512\pi^3}\left(1-\frac{m_Z^2}{m_h^2}\right)^3 \left| A_{\rm SM}^{Z\gamma} c_\beta - \frac{[\Sigma_a \mu_a]}{m_{k^{\pm\pm}}^2}\,(2Q_k g_{Zkk})\,A_0^{Z\gamma}(\tau_k^{\rm SM},\lambda_k)(-s_\beta)\right|^2, \tag{B.3}$$

$$\Gamma_{S'\to\gamma\gamma} = \frac{\alpha_{\rm EM}^2 m_{S'}^3}{256\pi^3 v^2}\left|\left(A_1^{\gamma\gamma}(\tau_{\rm W}) + N_C Q_t^2 A_{1/2}^{\gamma\gamma}(\tau_t)\right)s_\beta + \frac{1}{2}\frac{v[\Sigma_a\mu_a]}{m_{k^{\pm\pm}}^2} Q_k^2 A_0^{\gamma\gamma}(\tau_k)\,c_\beta\right|^2, \tag{B.4}$$

$$\Gamma_{S'\to Z\gamma} = \frac{\alpha_{\rm EM}^2 m_{S'}^3}{512\pi^3}\left(1-\frac{m_Z^2}{m_{S'}^2}\right)^3 \left| A_{\rm SM}^{Z\gamma}(\tau_{W,t}^{\rm SM}\to\tau_{W,t}) s_\beta - \frac{[\Sigma_a\mu_a]}{m_{k^{\pm\pm}}^2}\,(2Q_k g_{Zkk})\,A_0^{Z\gamma}(\tau_k,\lambda_k)\,c_\beta\right|^2, \tag{B.5}$$

$$\Gamma_{S'\to ZZ} = \left|\left(\Gamma_{\rm tot}(H_{750\,\rm GeV}^{\rm SM})\mathcal{B}(H_{750\,\rm GeV}^{\rm SM}\to ZZ)\right)^{1/2} s_\beta + \mathcal{M}_{S\to ZZ}\,c_\beta\right|^2, \tag{B.6}$$

with the factors

$$A_{\rm SM}^{Z\gamma} = \frac{2}{v}\left[\cot\theta_{\rm W} A_1^{Z\gamma}(\tau_{\rm W}^{\rm SM},\lambda_{\rm W}) + N_C\frac{(2Q_t)(T_3^{(t)}-2Q_t s_{\rm W}^2)}{s_{\rm W}c_{\rm W}} A_{1/2}^{Z\gamma}(\tau_t^{\rm SM},\lambda_t)\right], \tag{B.7}$$

$$\mathcal{M}_{S\to ZZ} = \left\{\left(\frac{s_W^2}{2c_W^2}\right)\frac{\alpha_{\rm EM}^2 m_{S'}^3}{512\pi^3}\left(1-\frac{m_Z^2}{m_{S'}^2}\right)^3\right\}^{1/2}\left[-\frac{[\Sigma_a\mu_a]}{m_{k^{\pm\pm}}^2}\,(2Q_k g_{Zkk})\,A_0^{Z\gamma}(\tau_k,\lambda_k)\right], \tag{B.8}$$

$$A_1^{\gamma\gamma}(x) = -x^2\left[2x^{-2}+3x^{-1}+3(2x^{-1}-1)f(x^{-1})\right], \tag{B.9}$$

$$A_{1/2}^{\gamma\gamma}(x) = 2x^2\left[x^{-1}+(x^{-1}-1)f(x^{-1})\right], \tag{B.10}$$

$$A_1^{Z\gamma}(x,y) = 4(3-\tan^2\theta_{\rm W})I_2(x,y) + \left[(1+2x^{-1})\tan^2\theta_{\rm W} - (5+2x^{-1})\right]I_1(x,y), \tag{B.11}$$

$$A_{1/2}^{Z\gamma}(x,y) = I_1(x,y) - I_2(x,y). \tag{B.12}$$

Here, the ratios and the two functions are defined for convenience:

$$\tau_i^{\rm SM} = \frac{4m_i^2}{m_h^2}, \quad \tau_i = \frac{4m_i^2}{m_{S'}^2} \quad (i=t,W,k), \tag{B.13}$$

$$I_1(x,y) = \frac{xy}{2(x-y)} + \frac{x^2y^2}{2(x-y)^2}\left[f(x^{-1})-f(y^{-1})\right] + \frac{x^2y}{(x-y)^2}\left[g(x^{-1})-g(y^{-1})\right]$$
$$= A_0^{Z\gamma}(x,y), \tag{B.14}$$

$$I_2(x,y) = -\frac{xy}{2(x-y)}\left[f(x^{-1})-f(y^{-1})\right]. \tag{B.15}$$

Here, α_s, $N_C\,(=3)$, $Q_t\,(=2/3)$, and $T_3^{(t)}\,(=1/2)$ are the fine structure constants of the QCD coupling, the QCD color factor for quarks, the electric charges of the top quark in units of the positron's one, and the weak isospin of the top quark, respectively. Other variables have already been defined around Eqs. (3.5)–(3.8). When we take the limit $s_\beta \to 0$, $\Gamma_{S'\to ZZ}$ is reduced to the form in Eq. (3.2).

Appendix C. Additional plots

In this appendix, we provide plots for discussing the case of the mixing of two fields S and Φ through mass terms under the assumption $\langle S\rangle = 0$ in Figs. C.1 and C.2. Here, the mass parameter $m_{S'h}$ in

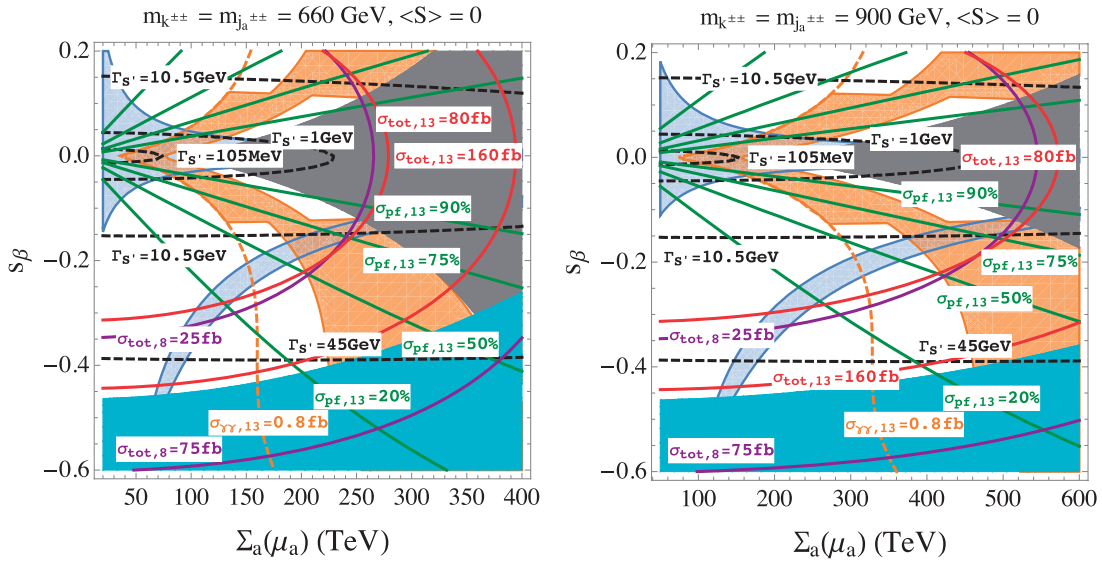

Fig. C.1. Allowed ranges of the parameters $\{\Sigma_a(\mu_a), s_\beta\}$ are shown in the two choices of the mass of the degenerate doubly charged scalars ($m_{k^{\pm\pm}}$ [$= m_{j_a^{\pm\pm}}$] $= 660/900$ GeV [left panel/right panel]). Under the assumption $\langle S \rangle = 0$, the value of $m_{S'h}$ is fixed as shown in Eq. (3.26). The light blue regions represent 2σ allowed regions of 125 GeV Higgs signal strengths, while the orange regions suggest the areas where the 750 GeV excess is suitably explained. The gray/cyan regions are excluded in 95% C.L.s by the ATLAS 8 TeV results for $S' \to \gamma\gamma/ZZ$. For a better understanding, several contours for the total width of S' ($\Gamma_{S'}$), total production cross sections at $\sqrt{s} = 8/13$ TeV ($\sigma_{\text{tot},8/13}$), and the percentage of the production through the photon fusion at $\sqrt{s} = 13$ TeV ($\sigma_{\text{pf},13}$) are illustrated.

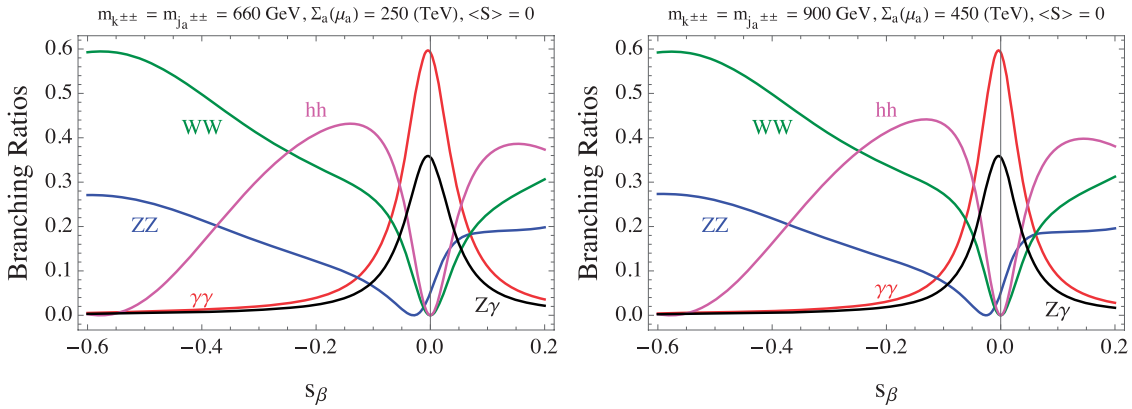

Fig. C.2. Relevant branching ratios of S' in the two configurations in Fig. C.1 are shown. Here, values of $\Sigma_a(\mu_a)$ are suitably fixed as typical digits in the corresponding allowed regions.

the S'-h-h interaction is automatically determined by the two mass eigenvalues and the mixing angle β as shown in Eq. (3.26). We note that the two choices in the universal mass of doubly charged scalars (660 GeV and 900 GeV) are from the expected 95% C.L. lower bounds under the assumption $\mathcal{B}(j_a^{\pm\pm} \to \mu^\pm\mu^\pm) = 100\%$ when $N_j = 10$ and $N_j = 100$, respectively.

References

[1] ATLAS Collaboration, Technical Report ATLAS-CONF-2015-081.
[2] CMS Collaboration, Technical Report CMS-PAS-EXO-15-004.
[3] ATLAS Collaboration, Technical Report ATLAS-CONF-2016-018.

[4] CMS Collaboration, Technical Report CMS-PAS-EXO-16-018.
[5] K. Harigaya and Y. Nomura, arXiv:1512.04850 [hep-ph] [Search INSPIRE].
[6] Y. Mambrini, G. Arcadi, and A. Djouadi, arXiv:1512.04913 [hep-ph] [Search INSPIRE].
[7] M. Backovic, A. Mariotti, and D. Redigolo, arXiv:1512.04917 [hep-ph] [Search INSPIRE].
[8] A. Angelescu, A. Djouadi, and G. Moreau, arXiv:1512.04921 [hep-ph] [Search INSPIRE].
[9] Y. Nakai, R. Sato, and K. Tobioka, arXiv:1512.04924 [hep-ph] [Search INSPIRE].
[10] S. Knapen, T. Melia, M. Papucci, and K. Zurek, arXiv:1512.04928 [hep-ph] [Search INSPIRE].
[11] D. Buttazzo, A. Greljo, and D. Marzocca, arXiv:1512.04929 [hep-ph] [Search INSPIRE].
[12] A. Pilaftsis, arXiv:1512.04931 [hep-ph] [Search INSPIRE].
[13] R. Franceschini, G. F. Giudice, J. F. Kamenik, M. McCullough, A. Pomarol, R. Rattazzi, M. Redi, F. Riva, A. Strumia, and R. Torre, arXiv:1512.04933 [hep-ph] [Search INSPIRE].
[14] S. Di Chiara, L. Marzola, and M. Raidal, arXiv:1512.04939 [hep-ph] [Search INSPIRE].
[15] T. Higaki, K. S. Jeong, N. Kitajima, and F. Takahashi, arXiv:1512.05295 [hep-ph] [Search INSPIRE].
[16] S. D. McDermott, P. Meade, and H. Ramani, arXiv:1512.05326 [hep-ph] [Search INSPIRE].
[17] J. Ellis, S. A. R. Ellis, J. Quevillon, V. Sanz, and T. You, arXiv:1512.05327 [hep-ph] [Search INSPIRE].
[18] M. Low, A. Tesi, and L.-T. Wang, arXiv:1512.05328 [hep-ph] [Search INSPIRE].
[19] B. Bellazzini, R. Franceschini, F. Sala, and J. Serra, arXiv:1512.05330 [hep-ph] [Search INSPIRE].
[20] R. S. Gupta, S. Jager, Y. Kats, G. Perez, and E. Stamou, arXiv:1512.05332 [hep-ph] [Search INSPIRE].
[21] C. Petersson and R. Torre, arXiv:1512.05333 [hep-ph] [Search INSPIRE].
[22] E. Molinaro, F. Sannino, and N. Vignaroli, arXiv:1512.05334 [hep-ph] [Search INSPIRE].
[23] A. Falkowski, O. Slone, and T. Volansky, arXiv:1512.05777 [hep-ph] [Search INSPIRE].
[24] B. Dutta, Y. Gao, T. Ghosh, I. Gogoladze, and T. Li, arXiv:1512.05439 [hep-ph] [Search INSPIRE].
[25] Q.-H. Cao, Y. Liu, K.-P. Xie, B. Yan, and D.-M. Zhang, arXiv:1512.05542 [hep-ph] [Search INSPIRE].
[26] S. Matsuzaki and K. Yamawaki, arXiv:1512.05564 [hep-ph] [Search INSPIRE].
[27] A. Kobakhidze, F. Wang, L. Wu, J. M. Yang, and M. Zhang, arXiv:1512.05585 [hep-ph] [Search INSPIRE].
[28] R. Martinez, F. Ochoa, and C. F. Sierra, arXiv:1512.05617 [hep-ph] [Search INSPIRE].
[29] P. Cox, A. D. Medina, T. S. Ray, and A. Spray, arXiv:1512.05618 [hep-ph] [Search INSPIRE].
[30] D. Becirevic, E. Bertuzzo, O. Sumensari, and R. Z. Funchal, arXiv:1512.05623 [hep-ph] [Search INSPIRE].
[31] J. M. No, V. Sanz, and J. Setford, arXiv:1512.05700 [hep-ph] [Search INSPIRE].
[32] S. V. Demidov and D. S. Gorbunov, arXiv:1512.05723 [hep-ph] [Search INSPIRE].
[33] W. Chao, R. Huo, and J.-H. Yu, arXiv:1512.05738 [hep-ph] [Search INSPIRE].
[34] S. Fichet, G. von Gersdorff, and C. Royon, arXiv:1512.05751 [hep-ph] [Search INSPIRE].
[35] D. Curtin and C. B. Verhaaren, arXiv:1512.05753 [hep-ph] [Search INSPIRE].
[36] L. Bian, N. Chen, D. Liu, and J. Shu, arXiv:1512.05759 [hep-ph] [Search INSPIRE].
[37] J. Chakrabortty, A. Choudhury, P. Ghosh, S. Mondal, and T. Srivastava, arXiv:1512.05767 [hep-ph] [Search INSPIRE].
[38] A. Ahmed, B. M. Dillon, B. Grzadkowski, J. F. Gunion, and Y. Jiang, arXiv:1512.05771 [hep-ph] [Search INSPIRE].
[39] P. Agrawal, J. Fan, B. Heidenreich, M. Reece, and M. Strassler, arXiv:1512.05775 [hep-ph] [Search INSPIRE].
[40] C. Csaki, J. Hubisz, and J. Terning, arXiv:1512.05776 [hep-ph] [Search INSPIRE].
[41] D. Aloni, K. Blum, A. Dery, A. Efrati, and Y. Nir, arXiv:1512.05778 [hep-ph] [Search INSPIRE].
[42] Y. Bai, J. Berger, and R. Lu, arXiv:1512.05779 [hep-ph] [Search INSPIRE].
[43] E. Gabrielli, K. Kannike, B. Mele, M. Raidal, C. Spethmann, and H. Veermae, arXiv:1512.05961 [hep-ph] [Search INSPIRE].
[44] R. Benbrik, C.-H. Chen, and T. Nomura, arXiv:1512.06028 [hep-ph] [Search INSPIRE].
[45] J. S. Kim, J. Reuter, K. Rolbiecki, and R. Ruiz de Austri, arXiv:1512.06083 [hep-ph] [Search INSPIRE].
[46] A. Alves, A. G. Dias, and K. Sinha, arXiv:1512.06091 [hep-ph] [Search INSPIRE].
[47] E. Megias, O. Pujolas, and M. Quiros, arXiv:1512.06106 [hep-ph] [Search INSPIRE].
[48] L. M. Carpenter, R. Colburn, and J. Goodman, arXiv:1512.06107 [hep-ph] [Search INSPIRE].
[49] J. Bernon and C. Smith, arXiv:1512.06113 [hep-ph] [Search INSPIRE].
[50] W. Chao, arXiv:1512.06297 [hep-ph] [Search INSPIRE].
[51] M. T. Arun and P. Saha, arXiv:1512.06335 [hep-ph] [Search INSPIRE].

[52] C. Han, H. M. Lee, M. Park, and V. Sanz, arXiv:1512.06376 [hep-ph] [Search INSPIRE].
[53] S. Chang, arXiv:1512.06426 [hep-ph] [Search INSPIRE].
[54] I. Chakraborty and A. Kundu, arXiv:1512.06508 [hep-ph] [Search INSPIRE].
[55] R. Ding, L. Huang, T. Li, and B. Zhu, arXiv:1512.06560 [hep-ph] [Search INSPIRE].
[56] H. Han, S. Wang, and S. Zheng, arXiv:1512.06562 [hep-ph] [Search INSPIRE].
[57] X.-F. Han and L. Wang, arXiv:1512.06587 [hep-ph] [Search INSPIRE].
[58] M.-x. Luo, K. Wang, T. Xu, L. Zhang, and G. Zhu, arXiv:1512.06670 [hep-ph] [Search INSPIRE].
[59] J. Chang, K. Cheung, and C.-T. Lu, arXiv:1512.06671 [hep-ph] [Search INSPIRE].
[60] D. Bardhan, D. Bhatia, A. Chakraborty, U. Maitra, S. Raychaudhuri, and T. Samui, arXiv:1512.06674 [hep-ph] [Search INSPIRE].
[61] T.-F. Feng, X.-Q. Li, H.-B. Zhang, and S.-M. Zhao, arXiv:1512.06696 [hep-ph] [Search INSPIRE].
[62] O. Antipin, M. Mojaza, and F. Sannino, arXiv:1512.06708 [hep-ph] [Search INSPIRE].
[63] F. Wang, L. Wu, J. M. Yang, and M. Zhang, arXiv:1512.06715 [hep-ph] [Search INSPIRE].
[64] J. Cao, C. Han, L. Shang, W. Su, J. M. Yang, and Y. Zhang, arXiv:1512.06728 [hep-ph] [Search INSPIRE].
[65] F. P. Huang, C. S. Li, Z. L. Liu, and Y. Wang, arXiv:1512.06732 [hep-ph] [Search INSPIRE].
[66] W. Liao and H.-q. Zheng, arXiv:1512.06741 [hep-ph] [Search INSPIRE].
[67] J. J. Heckman, arXiv:1512.06773 [hep-ph] [Search INSPIRE].
[68] M. Dhuria and G. Goswami, arXiv:1512.06782 [hep-ph] [Search INSPIRE].
[69] X.-J. Bi, Q.-F. Xiang, P.-F. Yin, and Z.-H. Yu, arXiv:1512.06787 [hep-ph] [Search INSPIRE].
[70] J. S. Kim, K. Rolbiecki, and R. R. de Austri, arXiv:1512.06797 [hep-ph] [Search INSPIRE].
[71] L. Berthier, J. M. Cline, W. Shepherd, and M. Trott, arXiv:1512.06799 [hep-ph] [Search INSPIRE].
[72] W. S. Cho, D. Kim, K. Kong, S. H. Lim, K. T. Matchev, J.-C. Park, and M. Park, arXiv:1512.06824 [hep-ph] [Search INSPIRE].
[73] J. M. Cline and Z. Liu, arXiv:1512.06827 [hep-ph] [Search INSPIRE].
[74] M. Bauer and M. Neubert, arXiv:1512.06828 [hep-ph] [Search INSPIRE].
[75] M. Chala, M. Duerr, F. Kahlhoefer, and K. Schmidt-Hoberg, arXiv:1512.06833 [hep-ph] [Search INSPIRE].
[76] D. Barducci, A. Goudelis, S. Kulkarni, and D. Sengupta, arXiv:1512.06842 [hep-ph] [Search INSPIRE].
[77] G. M. Pelaggi, A. Strumia, and E. Vigiani, arXiv:1512.07225 [hep-ph] [Search INSPIRE].
[78] S. M. Boucenna, S. Morisi, and A. Vicente, arXiv:1512.06878 [hep-ph] [Search INSPIRE].
[79] C. W. Murphy, arXiv:1512.06976 [hep-ph] [Search INSPIRE].
[80] A. E. Cárcamo Hernández and I. Nisandzic, arXiv:1512.07165 [hep-ph] [Search INSPIRE].
[81] U. K. Dey, S. Mohanty, and G. Tomar, arXiv:1512.07212 [hep-ph] [Search INSPIRE].
[82] J. de Blas, J. Santiago, and R. Vega-Morales, arXiv:1512.07229 [hep-ph] [Search INSPIRE].
[83] A. Belyaev, G. Cacciapaglia, H. Cai, T. Flacke, A. Parolini, and H. Serôdio, arXiv:1512.07242 [hep-ph] [Search INSPIRE].
[84] P. S. B. Dev and D. Teresi, arXiv:1512.07243 [hep-ph] [Search INSPIRE].
[85] W.-C. Huang, Y.-L. S. Tsai, and T.-C. Yuan, arXiv:1512.07268 [hep-ph] [Search INSPIRE].
[86] S. Moretti and K. Yagyu, arXiv:1512.07462 [hep-ph] [Search INSPIRE].
[87] K. M. Patel and P. Sharma, arXiv:1512.07468 [hep-ph] [Search INSPIRE].
[88] M. Badziak, arXiv:1512.07497 [hep-ph] [Search INSPIRE].
[89] S. Chakraborty, A. Chakraborty, and S. Raychaudhuri, arXiv:1512.07527 [hep-ph] [Search INSPIRE].
[90] Q.-H. Cao, S.-L. Chen, and P.-H. Gu, arXiv:1512.07541 [hep-ph] [Search INSPIRE].
[91] W. Altmannshofer, J. Galloway, S. Gori, A. L. Kagan, A. Martin, and J. Zupan, arXiv:1512.07616 [hep-ph] [Search INSPIRE].
[92] M. Cvetič, J. Halverson, and P. Langacker, arXiv:1512.07622 [hep-ph] [Search INSPIRE].
[93] J. Gu and Z. Liu, arXiv:1512.07624 [hep-ph] [Search INSPIRE].
[94] B. C. Allanach, P. S. B. Dev, S. A. Renner, and K. Sakurai, arXiv:1512.07645 [hep-ph] [Search INSPIRE].
[95] H. Davoudiasl and C. Zhang, arXiv:1512.07672 [hep-ph] [Search INSPIRE].
[96] N. Craig, P. Draper, C. Kilic, and S. Thomas, arXiv:1512.07733 [hep-ph] [Search INSPIRE].
[97] K. Das and S. K. Rai, arXiv:1512.07789 [hep-ph] [Search INSPIRE].
[98] K. Cheung, P. Ko, J. S. Lee, J. Park, and P.-Y. Tseng, arXiv:1512.07853 [hep-ph] [Search INSPIRE].
[99] J. Liu, X.-P. Wang, and W. Xue, arXiv:1512.07885 [hep-ph] [Search INSPIRE].

[100] J. Zhang and S. Zhou, arXiv:1512.07889 [hep-ph] [Search INSPIRE].
[101] J. A. Casas, J. R. Espinosa, and J. M. Moreno, arXiv:1512.07895 [hep-ph] [Search INSPIRE].
[102] L. J. Hall, K. Harigaya, and Y. Nomura, arXiv:1512.07904 [hep-ph] [Search INSPIRE].
[103] H. Han, S. Wang, and S. Zheng, arXiv:1512.07992 [hep-ph] [Search INSPIRE].
[104] J.-C. Park and S. C. Park, arXiv:1512.08117 [hep-ph] [Search INSPIRE].
[105] A. Salvio and A. Mazumdar, arXiv:1512.08184 [hep-ph] [Search INSPIRE].
[106] D. Chway, R. Dermíšek, T. H. Jung, and H. D. Kim, arXiv:1512.08221 [hep-ph] [Search INSPIRE].
[107] G. Li, Y.-n. Mao, Y.-L. Tang, C. Zhang, Y. Zhou, and S.-h. Zhu, arXiv:1512.08255 [hep-ph] [Search INSPIRE].
[108] M. Son and A. Urbano, arXiv:1512.08307 [hep-ph] [Search INSPIRE].
[109] Y.-L. Tang and S.-h. Zhu, arXiv:1512.08323 [hep-ph] [Search INSPIRE].
[110] H. An, C. Cheung, and Y. Zhang, arXiv:1512.08378 [hep-ph] [Search INSPIRE].
[111] J. Cao, F. Wang, and Y. Zhang, arXiv:1512.08392 [hep-ph] [Search INSPIRE].
[112] F. Wang, W. Wang, L. Wu, J. M. Yang, and M. Zhang, arXiv:1512.08434 [hep-ph] [Search INSPIRE].
[113] C. Cai, Z.-H. Yu, and H.-H. Zhang, arXiv:1512.08440 [hep-ph] [Search INSPIRE].
[114] Q.-H. Cao, Y. Liu, K.-P. Xie, B. Yan, and D.-M. Zhang, arXiv:1512.08441 [hep-ph] [Search INSPIRE].
[115] J. E. Kim, arXiv:1512.08467 [hep-ph] [Search INSPIRE].
[116] J. Gao, H. Zhang, and H. X. Zhu, arXiv:1512.08478 [hep-ph] [Search INSPIRE].
[117] W. Chao, arXiv:1512.08484 [hep-ph] [Search INSPIRE].
[118] X.-J. Bi, R. Ding, Y. Fan, L. Huang, C. Li, T. Li, S. Raza, X.-C. Wang, and B. Zhu, arXiv:1512.08497 [hep-ph] [Search INSPIRE].
[119] F. Goertz, J. F. Kamenik, A. Katz, and M. Nardecchia, arXiv:1512.08500 [hep-ph] [Search INSPIRE].
[120] L. A. Anchordoqui, I. Antoniadis, H. Goldberg, X. Huang, D. Lust, and T. R. Taylor, arXiv:1512.08502 [hep-ph] [Search INSPIRE].
[121] P. S. B. Dev, R. N. Mohapatra, and Y. Zhang, arXiv:1512.08507 [hep-ph] [Search INSPIRE].
[122] N. Bizot, S. Davidson, M. Frigerio, and J. L. Kneur, arXiv:1512.08508 [hep-ph] [Search INSPIRE].
[123] Y. Hamada, T. Noumi, S. Sun, and G. Shiu, arXiv:1512.08984 [hep-ph] [Search INSPIRE].
[124] S. Kanemura, N. Machida, S. Odori, and T. Shindou, arXiv:1512.09053 [hep-ph] [Search INSPIRE].
[125] Y. Jiang, Y.-Y. Li, and T. Liu, arXiv:1512.09127 [hep-ph] [Search INSPIRE].
[126] G. Aad et al., Phys. Rev. D **92**, 032004 [arXiv:1504.05511 [hep-ex]] [Search INSPIRE].
[127] CMS Collaboration, Technical Report CMS-PAS-HIG-14-006.
[128] https://twiki.cern.ch/twiki/bin/view/LHCPhysics/CERNYellowReportPageAt1314TeV2014.
[129] J. R. Andersen et al., arXiv:1307.1347 [hep-ph] [Search INSPIRE].
[130] G. Aad et al., Eur. Phys. J. C **76**, 45 (2016) [arXiv:1507.05930 [hep-ex]] [Search INSPIRE].
[131] A. Zee, Phys. Lett. B **93**, 389 (1980); **95**, 461 (1980) [erratum].
[132] T. P. Cheng and L.-F. Li, Phys. Rev. D **22**, 2860 (1980).
[133] A. Zee, Nucl. Phys. B **264**, 99 (1986).
[134] K. S. Babu, Phys. Lett. B **203**, 132 (1988).
[135] E. Ma, Phys. Rev. D **73**, 077301 (2006) [arXiv:hep-ph/0601225] [hep-ph] [Search INSPIRE].
[136] L. M. Krauss, S. Nasri, and M. Trodden, Phys. Rev. D **67**, 085002 (2003) [arXiv:hep-ph/0210389] [hep-ph] [Search INSPIRE].
[137] M. Aoki, S. Kanemura, and O. Seto, Phys. Rev. Lett. **102**, 051805 (2009) [arXiv:0807.0361 [hep-ph]] [Search INSPIRE].
[138] M. Aoki, S. Kanemura, and K. Yagyu, Phys. Rev. D **83**, 075016 (2011) [arXiv:1102.3412 [hep-ph]] [Search INSPIRE].
[139] M. Gustafsson, J. M. No, and M. A. Rivera, Phys. Rev. Lett. **110**, 211802 (2013); **112**, 259902 (2014) [erratum]; [arXiv:1212.4806 [hep-ph]] [Search INSPIRE].
[140] Y. Kajiyama, H. Okada, and K. Yagyu, J. High Energy Phys. **10**, 196 (2013) [arXiv:1307.0480 [hep-ph]] [Search INSPIRE].
[141] A. Ahriche, C.-S. Chen, K. L. McDonald, and S. Nasri, Phys. Rev. D **90**, 015024 (2014) [arXiv:1404.2696 [hep-ph]] [Search INSPIRE].
[142] A. Ahriche, K. L. McDonald, and S. Nasri, J. High Energy Phys. **10**, 167 (2014) [arXiv:1404.5917 [hep-ph]] [Search INSPIRE].
[143] C.-S. Chen, K. L. McDonald, and S. Nasri, Phys. Lett. B **734**, 388 (2014) [arXiv:1404.6033 [hep-ph]] [Search INSPIRE].

[144] H. Okada and Y. Orikasa, Phys. Rev. D **90**, 075023 (2014) [arXiv:1407.2543 [hep-ph]] [Search INSPIRE].
[145] H. Hatanaka, K. Nishiwaki, H. Okada, and Y. Orikasa, Nucl. Phys. B **894**, 268 (2015) [arXiv:1412.8664 [hep-ph]] [Search INSPIRE].
[146] L.-G. Jin, R. Tang, and F. Zhang, Phys. Lett. B **741**, 163 (2015) [arXiv:1501.02020 [hep-ph]] [Search INSPIRE].
[147] P. Culjak, K. Kumericki, and I. Picek, Phys. Lett. B **744**, 237 (2015) [arXiv:1502.07887 [hep-ph]] [Search INSPIRE].
[148] C.-Q. Geng, D. Huang, and L.-H. Tsai, Phys. Lett. B **745**, 56 (2015) [arXiv:1504.05468 [hep-ph]] [Search INSPIRE].
[149] A. Ahriche, K. L. McDonald, S. Nasri, and T. Toma, Phys. Lett. B **746**, 430 (2015) [arXiv:1504.05755 [hep-ph]] [Search INSPIRE].
[150] K. Nishiwaki, H. Okada, and Y. Orikasa, Phys. Rev. D **92**, 093013 (2015) [arXiv:1507.02412 [hep-ph]] [Search INSPIRE].
[151] H. Okada and K. Yagyu, arXiv:1508.01046 [hep-ph] [Search INSPIRE].
[152] A. Ahriche, K. L. McDonald, and S. Nasri, arXiv:1508.02607 [hep-ph] [Search INSPIRE].
[153] A. Ahriche, K. L. McDonald, and S. Nasri, Phys. Rev. D **92**, 095020 (2015) [arXiv:1508.05881 [hep-ph]] [Search INSPIRE].
[154] T. Nomura and H. Okada, Phys. Lett. B **755**, 306 (2016) [arXiv:1601.00386 [hep-ph]] [Search INSPIRE].
[155] T. Nomura and H. Okada, arXiv:1601.04516 [hep-ph] [Search INSPIRE].
[156] H. Okada and K. Yagyu, Phys. Lett. B **756**, 337 (2016) [arXiv:1601.05038 [hep-ph]] [Search INSPIRE].
[157] T. Nomura and H. Okada, Phys. Lett. B **756**, 295 (2016) [arXiv:1601.07339 [hep-ph]] [Search INSPIRE].
[158] C. Arbeláez, A. E. Cárcamo Hernández, S. Kovalenko, and I. Schmidt, arXiv:1602.03607 [hep-ph] [Search INSPIRE].
[159] P. Ko, T. Nomura, H. Okada, and Y. Orikasa, arXiv:1602.07214 [hep-ph] [Search INSPIRE].
[160] S. C. Park and Ji. Shu, Phys. Rev. D **79**, 091702 (2009) [arXiv:0901.0720 [hep-ph]] [Search INSPIRE].
[161] C.-R. Chen, M. M. Nojiri, S. C. Park, J. Shu, and M. Takeuchi, J. High Energy Phys. **09**, 078 (2009) [arXiv:0903.1971 [hep-ph]] [Search INSPIRE].
[162] C.-R. Chen, M. M. Nojiri, S. C. Park, and J. Shu, arXiv:0908.4317 [hep-ph] [Search INSPIRE].
[163] S. C. Park and J. Shu, AIP Conf. Proc. **1200**, 587 (2010) [arXiv:0910.0931 [hep-ph]] [Search INSPIRE].
[164] K. Kong, S. C. Park, and T. G. Rizzo, J. High Energy Phys. **04**, 081 (2010) [arXiv:1002.0602 [hep-ph]] [Search INSPIRE].
[165] K. Kong, S. C. Park, and T. G. Rizzo, J. High Energy Phys. **07**, 059 (2010) [arXiv:1004.4635 [hep-ph]] [Search INSPIRE].
[166] C. Csaki, J. Heinonen, J. Hubisz, S. C. Park, and J. Shu, J. High Energy Phys. **01**, 089 (2011) [arXiv:1007.0025 [hep-ph]] [Search INSPIRE].
[167] K. Nishiwaki, J. High Energy Phys. **05**, 111 (2012) [arXiv:1101.0649 [hep-ph]] [Search INSPIRE].
[168] K. Nishiwaki, K.-y. Oda, N. Okuda, and R. Watanabe, Phys. Lett. B **707**, 506 (2012) [arXiv:1108.1764 [hep-ph]] [Search INSPIRE].
[169] K. Nishiwaki, K.-y. Oda, N. Okuda, and R. Watanabe, Phys. Rev. D **85**, 035026 (2012) [arXiv:1108.1765 [hep-ph]] [Search INSPIRE].
[170] D. Kim, Y. Oh, and S. C. Park, J. Korean Phys. Soc. **67**, 1137 (2015) [arXiv:1109.1870 [hep-ph]] [Search INSPIRE].
[171] A. K. Datta, K. Nishiwaki, and S. Niyogi, J. High Energy Phys. **11**, 154 (2012) [arXiv:1206.3987 [hep-ph]] [Search INSPIRE].
[172] T. Flacke, K. Kong, and S. C. Park, J. High Energy Phys. **05**, 111 (2013) [arXiv:1303.0872 [hep-ph]] [Search INSPIRE].
[173] T. Kakuda, K. Nishiwaki, K.-y. Oda, and R. Watanabe, Phys. Rev. D **88**, 035007 (2013) [arXiv:1305.1686 [hep-ph]] [Search INSPIRE].
[174] T. Flacke, K. Kong, and S. C. Park, Phys. Lett. B **728**, 262 (2014) [arXiv:1309.7077 [hep-ph]] [Search INSPIRE].

[175] A. K. Datta, K. Nishiwaki, and S. Niyogi, J. High Energy Phys. **01**, 104 (2014) [arXiv:1310.6994 [hep-ph]] [Search INSPIRE].
[176] H. Dohi, T. Kakuda, K. Nishiwaki, K.-y. Oda, and N. Okuda, Afr. Rev. Phys. **9**, 0069 (2014) [arXiv:1406.1954 [hep-ph]] [Search INSPIRE].
[177] T. Flacke, K. Kong, and S. C. Park, Mod. Phys. Lett. **A30**, 1530003 (2015) [arXiv:1408.4024 [hep-ph]] [Search INSPIRE].
[178] H. M. Lee, D. Kim, K. Kong, and S. C. Park, J. High Energy Phys. **11**, 150 (2015) [arXiv:1507.06312 [hep-ph]] [Search INSPIRE].
[179] J. R. Ellis, M. K. Gaillard, and D. V. Nanopoulos, Nucl. Phys. B **106**, 292 (1976).
[180] M. A. Shifman, A. I. Vainshtein, M. B. Voloshin, and V. I. Zakharov, Sov. J. Nucl. Phys. **30**, 711 (1979).
[181] M. A. Shifman, A. I. Vainshtein, M. B. Voloshin, and V. I. Zakharov, Yad. Fiz. **30**, 1368 (1979).
[182] A. Djouadi, Phys. Rept. **457**, 1 (2008) [arXiv:hep-ph/0503172 [hep-ph]] [Search INSPIRE].
[183] M. Carena, I. Low, and C. E. M. Wagner, J. High Energy Phys. **08**, 060 (2012) [arXiv:1206.1082 [hep-ph]] [Search INSPIRE].
[184] C.-S. Chen, C.-Q. Geng, D. Huang, and L.-H. Tsai, Phys. Rev. D **87**, 075019 (2013) [arXiv:1301.4694 [hep-ph]] [Search INSPIRE].
[185] L. A. Harland-Lang, V. A. Khoze, and M. G. Ryskin, J. High Energy Phys. **03**, 182 (2016) [arXiv:1601.07187 [hep-ph]] [Search INSPIRE].
[186] A. D. Martin and M. G. Ryskin, Eur. Phys. J. C **74**, 3040 (2014) [arXiv:1406.2118 [hep-ph]] [Search INSPIRE].
[187] U. Danielsson, R. Enberg, G. Ingelman, and T. Mandal, arXiv:1601.00624 [hep-ph] [Search INSPIRE].
[188] C. Csaki, J. Hubisz, S. Lombardo, and J. Terning, [arXiv:1601.00638 [hep-ph]] [Search INSPIRE].
[189] H. Ito, T. Moroi, and Y. Takaesu, Phys. Lett. B **756**, 147 (2016) [arXiv:1601.01144 [hep-ph]] [Search INSPIRE].
[190] F. D'Eramo, J. de Vries, and P. Panci, arXiv:1601.01571 [hep-ph] [Search INSPIRE].
[191] I. Sahin, arXiv:1601.01676 [hep-ph] [Search INSPIRE].
[192] S. Fichet, G. von Gersdorff, and C. Royon, arXiv:1601.01712 [hep-ph] [Search INSPIRE].
[193] L. A. Harland-Lang, V. A. Khoze, and M. G. Ryskin, arXiv:1601.03772 [hep-ph] [Search INSPIRE].
[194] D. B. Franzosi and M. T. Frandsen, arXiv:1601.05357 [hep-ph] [Search INSPIRE].
[195] S. Abel and V. V. Khoze, arXiv:1601.07167 [hep-ph] [Search INSPIRE].
[196] I. Ben-Dayan and R. Brustein, arXiv:1601.07564 [hep-ph] [Search INSPIRE].
[197] A. D. Martin and M. G. Ryskin, J. Phys. G **43**, 04LT02 (2016) [arXiv:1601.07774 [hep-ph]] [Search INSPIRE].
[198] N. D. Barrie, A. Kobakhidze, M. Talia, and L. Wu, Phys. Lett. B **755**, 343 (2016) [arXiv:1602.00475 [hep-ph]] [Search INSPIRE].
[199] H. Ito, T. Moroi, and Y. Takaesu, arXiv:1602.01231 [hep-ph] [Search INSPIRE].
[200] C. Gross, O. Lebedev, and J. M. No, arXiv:1602.03877 [hep-ph] [Search INSPIRE].
[201] S. Baek and J.-h. Park, arXiv:1602.05588 [hep-ph] [Search INSPIRE].
[202] E. Molinaro, F. Sannino, and N. Vignaroli, arXiv:1602.07574 [hep-ph] [Search INSPIRE].
[203] G. Panico, L. Vecchi, and A. Wulzer, arXiv:1603.04248 [hep-ph] [Search INSPIRE].
[204] A. Bharucha, A. Djouadi, and A. Goudelis, arXiv:1603.04464 [hep-ph] [Search INSPIRE].
[205] M. Ababekri, S. Dulat, J. Isaacson, C. Schmidt, and C. P. Yuan, arXiv:1603.04874 [hep-ph] [Search INSPIRE].
[206] L. A. Anchordoqui, I. Antoniadis, H. Goldberg, X. Huang, D. Lust, and T. R. Taylor, arXiv:1603.08294 [hep-ph] [Search INSPIRE].
[207] K. Howe, S. Knapen, and D. J. Robinson, arXiv:1603.08932 [hep-ph] [Search INSPIRE].
[208] M. T. Frandsen and I. M. Shoemaker, arXiv:1603.09354 [hep-ph] [Search INSPIRE].
[209] C. F. Von Weizsacker, Z. Phys. **88**, 612 (1934).
[210] E. J. Williams, Phys. Rev. **45**, 729 (1934).
[211] G. Aad et al., Phys. Lett. B **738**, 428 (2014) [arXiv:1407.8150 [hep-ex]] [Search INSPIRE].
[212] ATLAS Collaboration, Technical Report ATLAS-CONF-2016-010.
[213] ATLAS Collaboration, Technical Report ATLAS-CONF-2016-016.
[214] G. Aad et al., J. High Energy Phys. **01**, 032 (2016) [arXiv:1509.00389 [hep-ex]] [Search INSPIRE].
[215] ATLAS Collaboration, Technical Report ATLAS-CONF-2014-005.

[216] J. F. Kamenik, B. R. Safdi, Y. Soreq, and J. Zupan, arXiv:1603.06566 [hep-ph] [Search INSPIRE].
[217] A. Schuessler and D. Zeppenfeld, SUSY 2007 Proc., 15th Int. Conf. Supersymmetry and Unification of Fundamental Interactions, July 26–August 1, 2007, Karlsruhe, Germany (2007) [arXiv:0710.5175 [hep-ph]] [Search INSPIRE].
[218] G. Aad et al., J. High Energy Phys. **03**, 041 (2015) [arXiv:1412.0237 [hep-ex]] [Search INSPIRE].
[219] J. Alwall, M. Herquet, F. Maltoni, O. Mattelaer, and T. Stelzer, J. High Energy Phys. **06**, 128 (2011) [arXiv:1106.0522 [hep-ph]] [Search INSPIRE].
[220] J. Alwall, R. Frederix, S. Frixione, V. Hirschi, F. Maltoni, O. Mattelaer, H. S. Shao, T. Stelzer, P. Torrielli, and M. Zaro, J. High Energy Phys. **07**, 079 (2014) [arXiv:1405.0301 [hep-ph]] [Search INSPIRE].
[221] N. D. Christensen and C. Duhr, Comput. Phys. Commun. **180**, 1614 (2009) [arXiv:0806.4194 [hep-ph]] [Search INSPIRE].
[222] A. Alloul, N. D. Christensen, C. Degrande, C. Duhr, and B. Fuks, Comput. Phys. Commun. **185**, 2250 (2014) [arXiv:1310.1921 [hep-ph]] [Search INSPIRE].
[223] C. Degrande, C. Duhr, B. Fuks, D. Grellscheid, O. Mattelaer, and T. Reiter, Comput. Phys. Commun. **183**, 1201 (2012) [arXiv:1108.2040 [hep-ph]] [Search INSPIRE].
[224] J. Pumplin, D. R. Stump, J. Huston, H. L. Lai, P. M. Nadolsky, and W. K. Tung, J. High Energy Phys. **07**, 012 (2002) [arXiv:hep-ph/0201195 [hep-ph]] [Search INSPIRE].
[225] D. S. M. Alves, J. Galloway, J. T. Ruderman, and J. R. Walsh, J. High Energy Phys. **02**, 007 (2015) [arXiv:1410.6810 [hep-ph]] [Search INSPIRE].
[226] D. Becciolini, M. Gillioz, M. Nardecchia, F. Sannino, and M. Spannowsky, Phys. Rev. D **91**, 015010 (2015); **92**, 079905 (2015) [erratum] [arXiv:1403.7411 [hep-ph]] [Search INSPIRE].
[227] K. J. Bae, M. Endo, K. Hamaguchi, and T. Moroi, arXiv:1602.03653 [hep-ph] [Search INSPIRE].
[228] S. Kanemura, Y. Okada, E. Senaha, and C. P. Yuan, Phys. Rev. D **70**, 115002 (2004) [arXiv:hep-ph/0408364 [hep-ph]] [Search INSPIRE].
[229] S. Dittmaier et al., arXiv:1101.0593 [hep-ph] [Search INSPIRE].
[230] S. Dittmaier et al., arXiv:1201.3084 [hep-ph] [Search INSPIRE].
[231] G. Aad et al., Phys. Rev. D **91**, 012006 (2015) [arXiv:1408.5191 [hep-ex]] [Search INSPIRE].
[232] G. Aad et al., Phys. Rev. D **90**, 112015 (2014) [arXiv:1408.7084 [hep-ex]] [Search INSPIRE].
[233] G. Aad et al., J. High Energy Phys. **01**, 069 (2015) [arXiv:1409.6212 [hep-ex]] [Search INSPIRE].
[234] ATLAS Collaboration, Technical Report ATLAS-CONF-2014-061.
[235] G. Aad et al., Phys. Rev. D **92**, 012006 (2015) [arXiv:1412.2641 [hep-ex]] [Search INSPIRE].
[236] V. Khachatryan et al., Eur. Phys. J. C **75**, 212 (2015) [arXiv:1412.8662 [hep-ex]] [Search INSPIRE].
[237] S. Kanemura, Y. Okada, and E. Senaha, Phys. Lett. B **606**, 361 (2005) [arXiv:hep-ph/0411354 [hep-ph]] [Search INSPIRE].
[238] ATLAS Collaboration, Technical Report ATLAS-CONF-2016-059.
[239] CMS Collaboration, Technical Report CMS-PAS-EXO-16-027.
[240] B. Fuks, D. W. Kang, S. C. Park, and M.-S. Seo, Phys. Lett. B **761**, 344 (2016) [arXiv:1608.00084 [hep-ph]] [Search INSPIRE].